AFRL-VS-TR-2001-1606

Experimental Demonstration of Underground Structure Characterization Using Sensitive Magnetic Sensors

Suman Ganguly

Center for Remote Sensing, Inc.
11350 Random Hills Rd., Suite 710
Fairfax, VA 22030

20 Nov. 2000

Final Report

AIR FORCE RESEARCH LABORATORY
Space Vehicles Directorate
29 Randolph Rd
AIR FORCE MATERIEL COMMAND
Hanscom AFB, MA 01731-3010

20021015 044

"This technical report has been reviewed and is approved for publication"

JAMES C. BATTIS
Contract Manager

Major CARL CHRISTENSEN
Acting Branch Chief

REPORT DOCUMENTATION PAGE

Form Approved
OMB No. 0704-0188

The public reporting burden for this collection of information is estimated to average 1 hour per response, including the time for reviewing instructions, searching existing data sources, gathering and maintaining the data needed, and completing and reviewing the collection of information. Send comments regarding this burden estimate or any other aspect of this collection of information, including suggestions for reducing the burden, to Department of Defense, Washington Headquarters Services, Directorate for Information Operations and Reports (0704-0188), 1215 Jefferson Davis Highway, Suite 1204, Arlington, VA 22202-4302. Respondents should be aware that notwithstanding any other provision of law, no person shall be subject to any penalty for failing to comply with a collection of information if it does not display a currently valid OMB control number.
PLEASE DO NOT RETURN YOUR FORM TO THE ABOVE ADDRESS.

1. REPORT DATE (DD-MM-YYYY)	2. REPORT TYPE	3. DATES COVERED (From - To)
20 Nov. 2000	Scientific, Final	18 Feb. 1998 - 20 Nov. 2000

4. TITLE AND SUBTITLE

Experimental Demonstration Under Structure Characterization Using Sensitive Magnetic Sensors

5a. CONTRACT NUMBER
F19628-98-C-0015

5b. GRANT NUMBER

5c. PROGRAM ELEMENT NUMBER
63160D

6. AUTHOR(S)

Suman Ganguly

5d. PROJECT NUMBER
4268

5e. TASK NUMBER
SD

5f. WORK UNIT NUMBER
AA

7. PERFORMING ORGANIZATION NAME(S) AND ADDRESS(ES)

Center for Remote Sensing
11350 Random Hills Rd.
Fairfax, VA 22020

8. PERFORMING ORGANIZATION REPORT NUMBER

9. SPONSORING/MONITORING AGENCY NAME(S) AND ADDRESS(ES)

Air Force Reserach Laboratory
20 Randolph Rd.
Hanscom, AFB, MA 01731-3010

10. SPONSOR/MONITOR'S ACRONYM(S)
AFRL/VSBXI

11. SPONSOR/MONITOR'S REPORT NUMBER(S)
AFRL-VS-TR-2001-1606

12. DISTRIBUTION/AVAILABILITY STATEMENT

Approved for public release, Distribution Unlimited

13. SUPPLEMENTARY NOTES

This work is sponosored by the Defense Threat Reduction Agency under DTRA MIPR#99-20999, and Work Unit 00748

14. ABSTRACT

Detection and characterization of various underground facilities using ELF/VLF signals generated by HAARP as well as from other sources are invetigated. A novel 3-D E.M. code has been used for simulation using arbitrary shaped facilities and under arbitrary ground. Results of the simulation are extremely promising.

Design of suitable sensors for E.M. detection has been performed. Plans for further development are made. For immediate applications a composite integrated with availble sensors has been made available. They system allows detection and real-time analysis using sophisticated signal processing techniques.

15. SUBJECT TERMS

Underground Structure, Characterization, Electromagnetic Sounding, Low Frequency, E.M., Magnetics

16. SECURITY CLASSIFICATION OF:			17. LIMITATION OF ABSTRACT	18. NUMBER OF PAGES	19a. NAME OF RESPONSIBLE PERSON
a. REPORT	b. ABSTRACT	c. THIS PAGE	SAR	50	James Battis
Unclassified	Unclassified	Unclassified			19b. TELEPHONE NUMBER (Include area code) (781) 377 - 4669

Standard Form 298 (Rev. 8/98)
Prescribed by ANSI Std. Z39.18

CONTENTS

1. INTRODUCTION AND BACKGROUND

Detection and characterization of deeply buried targets can be performed using the anomalies caused by void space, by their secondary effects or by the effects produced through materials with the target (see Table 1). Remote detection of associated activities and secondary effects may also be used as useful clues. Technical detection methods include: E.M. wave propagation, electric current flow, E.M. induction, magnetic filed and gravitational anomalies, seismic wave propagation, heat flow, in situ probes, etc. (see Table 2). Both active and passive techniques might be used and the sensors could be deployed using airborne, surface and sub-surface techniques.

For broad area detection airborne and surface and/or subsurface techniques may be considered. Anomalies caused by gravity, heat flow, etc. Are generally too small to be used for remote sensing using satellites or high flying aircraft. Magnetic and electromagnetic field techniques show promise for airborne as well as for ground based deployment. For ground based deployment concepts similar to networked ground sensors may be used, where the deployment could be performed by dropping the sensors from UAV or other types of vehicles.

TABLE 1
EM CHARACTERISITCS OF UNDERGROUND FACILITIES

Void in conductivity, dielectric constant, and magnetic permittivity
Presence of electrical and magnetic material in the UGF:

> Cables
> Equipment, drills, air-conditioner, blowers, fans, water pumps, coolers, transformers, generators.
> Metal Structures, Doors, Beams, Metal bars, Linings, rail tracks, processing facilities, etc.
> Ferrous material producing magnetic signatures, generators, transformers, iron beams, rail tracks.
> Nonlinearity through magnetic signatures.

EMMISIONS USABLE BY PASSIVE SENSORS:

All facilities are supplied with power. Both dc and ac power lines produce significant characteristics. Power transmission, distribution and return lines radiate according to the load. Most machinery and appliances radiate and vibrate at characteristic frequencies (generally in the few Hz range).

> Machinery loading results in radiation of power harmonics and load transients
> Grounding systems produces large currents throughout the region
> Magnetic field perturbations are indicative of load activities
> Modulations can be used to characterize different activities and sources (machinery types, make).
> Diesel generators and transformers provide various spectral characteristics which indicate their sources, manufactures and operating conditions.

Magnetic and electromagnetic sensors can use both active and passive techniques. Sensing of the earth's magnetic filed at different locations provides information about the magnetic anomaly created by magnetic and ferrous objects. Tunnel lining, concrete structures, etc., contain strong ferrous objects, which could be detected at distances/depths of more than 100 meters or so.

Various sources exist for low frequency anomaly detection. These include extreme low frequency fields produced by magnetospheric currents (magnetotelluric) covering the frequency range from almost dc to about 4-10 Hz. Lightning and other sources covering frequency bands of several KHz also exist. Notable among them are the VLF transmitters operating in the 10-25 KHz range and distributed throughout the world.

1

Controlled source electromagnetic sounding in the frequency range of 5 – 30 kHz has been used by geophysicists. The source could be airborne or can be deployed at the ground surface. Sensors can also be either airborne or deployed in the ground.

Underground deployment (using boreholes) of excitors and sensors is well known for geophysical exploration. They have generally been used for localized applications. The range of applications needs to be investigated using numerical simulation. (See earlier report)

Various techniques have been proposed for the detection, characterization and imaging of buried underground facilities. Evaluation of these techniques and the determination of their effectiveness under different conditions are essential for mission design, estimation and monitoring of the state of the target before and after the action. A wide variety of situations involving a broad rang of detection techniques, sensors and deployment scenarios can occur in practice; also, the targets of interest can be versatile in nature and be buried under terrain conditions. Thus, it is essential to have a versatile simulation tool that can model these scenarios in an efficient and accurate manner, and also be user-friendly. Furthermore, the reliability of the tool must be established by validating the results generated. The availability of such a tool would enable use to simulate a wide spectrum of scenarios, and generate a database that would be extremely useful for solving the inverse scattering problem, or that of imaging the underground structure. In addition, the tool would assist us in drawing valuable inferences regarding the activities, state and character of the target. An examination of the simulation results will also allow us to determine the system requirements, viz., the nature of the source, the sensor, and the modes of their deployments.

Recently a novel 3-D modeling code has been developed at CRS (Center for Remote Sensing) for accurate estimation of scattered fields over a wide range of frequencies. As mentioned earlier, this is the first code of its kind that can cover a wide range of frequencies (even down to near zero), and yet can accommodate a fine mesh to model the underground structure in fine detail. However, unlike the existing codes that suffer from convergence problems at low frequencies, e.g., below 500 Hz, the CRS code not only overcomes this barrier, but also performs the computations accurately without placing a severe burden on the CPU time and memory.

When fully developed, the comprehensive 3-D EM code would be useful for determining the perturbation effects introduced by various underground objects on the electromagnetic signals propagating above the interface. It is obvious that, in order to accommodate the wide range of targets, terrains, excitation sources, receiver types and deployment strategies, it will be imperative for us to develop a comprehensive, flexible, accurate, and user-friendly 3-D modeling tool that can handle a wide range of frequencies, various target sizes, geometries, and depths, different ground conductivities and permeabilities, inhomogeneties, stratification geometries and tilts. Different types of source excitations to be incorporated in this code are: plane wave (with an appropriate tilt for the finite ground conductivity); electric dipole with an arbitrary polarization; and, magnetic dipole, also with an arbitrary polarization. In addition, it will be necessary to be able to position these dipole excitations somewhat arbitrarily so as to have the desired flexibility in the measurement schemes. They may, for instance, be located anywhere on the surface of the ground, be above the ground (surveyed via the use of a UAV, aircraft, aerostat, etc.), or even be buried inside the ground. Excitations of the ground itself, through large currents produced by a long wire with ends deeply immersed in the ground, will also be modeled. Yet another class of sources that would be included in the model are emissions originating from the underground activities. These would include ac power lines, machinery generating associated power line harmonics, low frequency noises and radio emissions.

It is important to realize that adequate modeling of the detailed geometries of the underground structure will be necessary in order to enhance our identification capabilities. The presence of electric and magnetic materials inside the underground structures can produce strong signatures all the way down to D.C. (magnetic filed perturbation produced through ferrous materials). Magnetic materials can also produce significant nonlinearities in the scattered field. The nonlinear signatures can provide valuable information about the underground structure and activities. These signatures are to be used for imaging the underground structures and drawing valuable inferences about the nature, state and conditions of the underground activities.

The code must allow the field sensors to be deployed arbitrarily, i.e., aboveground, on the surface, or at underground locations. Since the primary application of the code would be to evaluate the effects of the underground targets though EM field effects, it should be able to compute the electric and magnetic field components at arbitrary locations. Once these filed perturbations introduced by various targets, emitting sources, and receiver locations are properly analyzed, the inversion techniques would not only enable us to image the underground cavities, but would also make it possible for an expert system (or experts) to analyze the data and derive inferences about the underground activities.

A thorough understanding of the effects of various targets on different sensors requires detailed simulations for a wide variety of situations and conditions. We have performed simulations using this code, with the objective of defining the sensor requirements, developing appropriate sensor and performing a field experiment.

The Center for Remote Sensing has developed a variety of extremely sensitive magnetic sensors, including both the fluxgate and induction coil types. Currently, the fluxgate sensors operate in the dc to tens of Hz range. Induction coils, on the other hand, could be extended down to a fraction of a Hz, but they become prohibitively bulky when operating at such low frequencies. The ideal situation would be to extend the operational frequency of fluxgates to around 1 kHz, and to employ the induction coils for frequencies above 1 kHz. This combination will provide a compact, sensitive system that is suitable for field demonstration. The proposed sensors would represent the utmost sensitivity and compactness achievable by using the currently available technology (see Interim Report). These sensors will be useful for accessing the detectability of specific targets under diverse conditions. This approach would also provide a baseline that would enable us to estimate the effectiveness of certain missions. Furthermore, it would allow an immediate use of such a system for operational purposes.

2. PRELIMINARY ANALYSIS

Our primary objective is to demonstrate the concept of extension of the FDTD technique to arbitrarily low frequencies.

Results of the simulations presented below clearly demonstrate that significant field perturbation is produce by an empty bunker. Some preliminary analysis has also been performed with the objective of finding absolute perturbations, stand off distance and the possibility of using magnetic field and measurements. These simulations have been performed using FDTD for frequencies above 1 kHz. These are shown in Figure 1 through Figure 8 in the present section. The two sets of geometries are used and are shown in Figure 1. All computations are made for two frequencies, i.e., 1 kHz and 10 kHz. Both plane wave field and Magnetic Loop excitation are used. The magnetic loop is placed 80 m to the left of the bunker. Received field components are calculated at 30, 70, and 110 m above ground. Figures 2, 3, 4, and 5 show the field perturbation due to the bunker. Field distributions above the source are shown in Figure 6 through 8.

For plane wave incidence, H_y is the dominant filed (see Figure 2, second panel in the left-hand column), where the perturbation due to bunker is observed. The perturbation is about 1% at 30 m above ground. The field falls off at almost R^{-2} with height. Thus for a plane wave of 1 gamma (i.e. 10^{-5} Gauss), the perturbation will be 10^{-7} gauss. This is detectable with our sensors.

Perturbations shown in the above mentioned panel refers to the field changes along the direction of E.M. wave propagation (x direction), which is also along the length of the tunnel (see Figure 1). For field components along the y direction (across the tunnel), the dominant file perturbation is caused by the vertical magnetic field component, e.g. H_z (see Figure 2; 3rd panel in the right hand column). Strong dHz dy values are also evident.

The Hz values remain strong even for a higher frequency of 10 kHz (see Figure 3, 3rd panel in the right hand column). The Hy component, however, drops to very small magnitude. These results clearly demonstrate the complexities of the geometry and orientation even for a plan wave situation. This further emphasizes the need for 3-D modeling and inadequacy of extrapolation of 2-D models.

For a dipole source the filed perturbation is more complicated. The typical perturbation is 10^{-3} to 10^{-4} parts. However, modest sources can be placed in nearby region to produce detectable field strengths.

Simulations have been performed using both plan wave source and dipole sources. Homogenous ground is used for all these simulations. The typical geometry is showing in Figure 1 in the Appendix. A bunker is modeled as a cavity typically 22.5 m x 20 m x 20 m.

Figures 2 and 3 describe the magnetic field components above the bunker. The measurements are made at the surface (blue dots). Figures 8 and 9 describe the field inside the bunker and Figure 10 shows the scattered field from the bunker.

The sharp gradients in the field are evident in Figures 15 and 16, where the H_x and H_y are measured 1m above the ground.

The software allows us to extend the frequency range down to almost dc. Some results of plane wave excitation at 10 Hz are shown in Figure 17. These may be compared with similar results for 100 kHz shown in Figure 18.
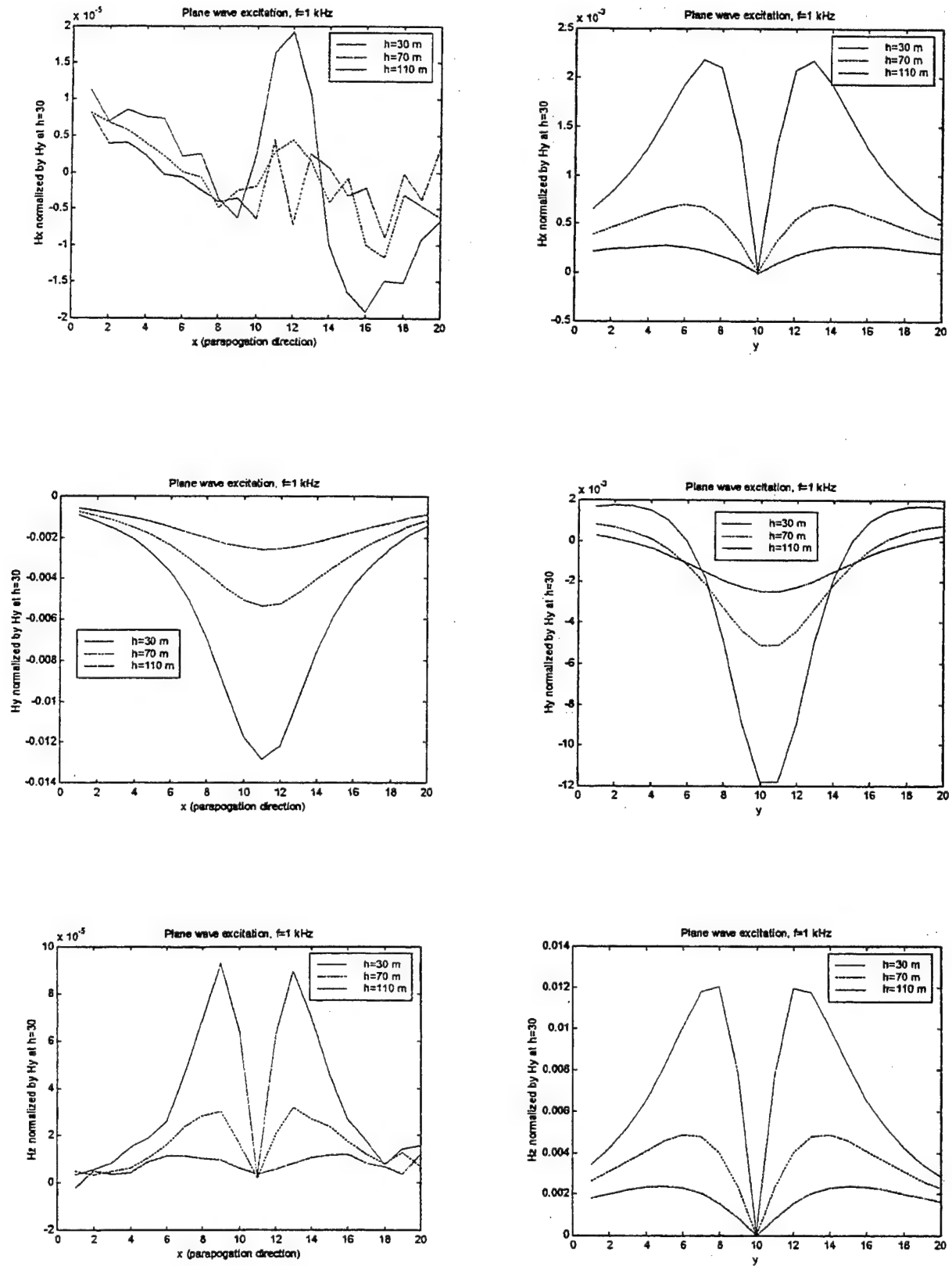
FIGURE CAPTIONS:

Figure 1   Geometry of the bunker problem.

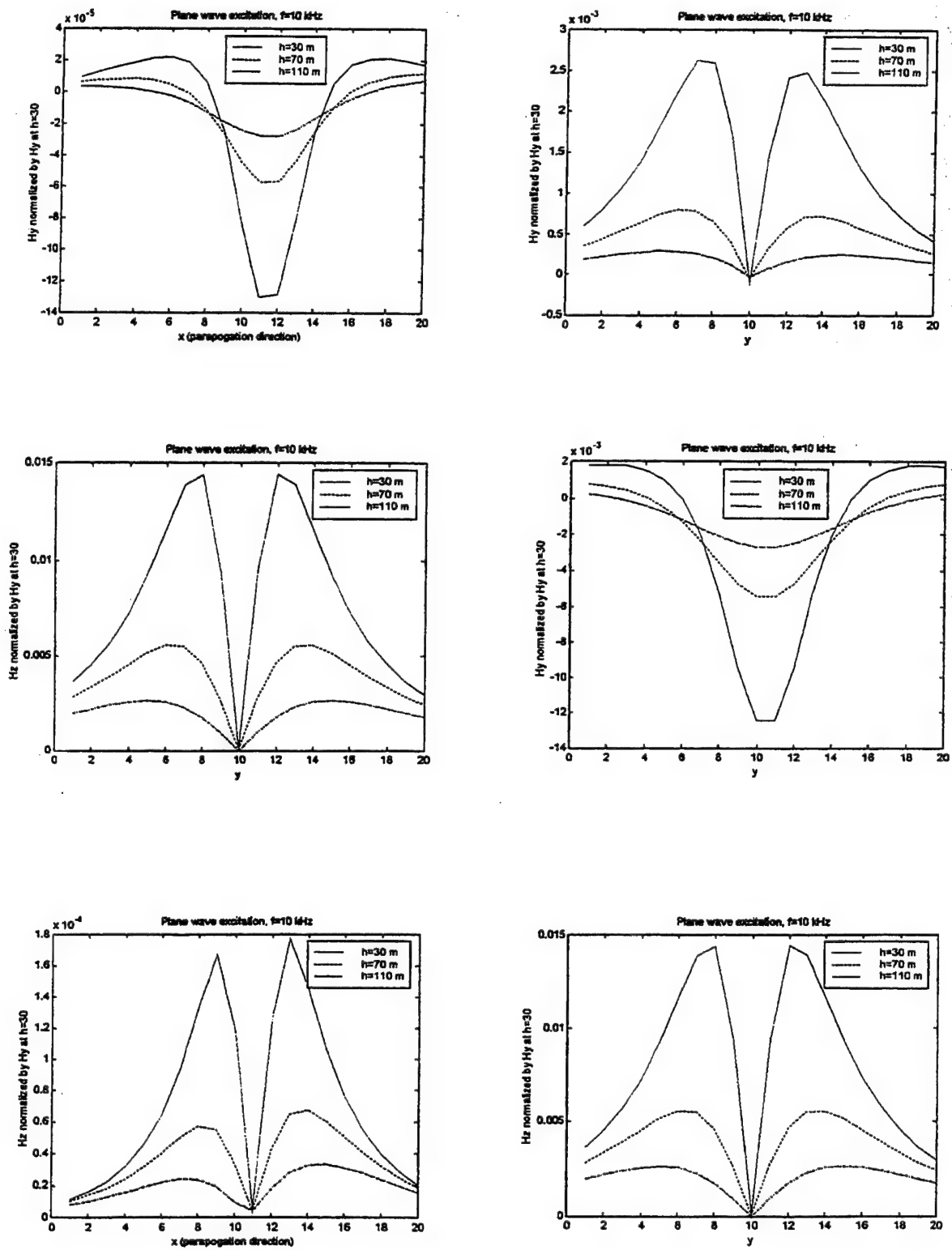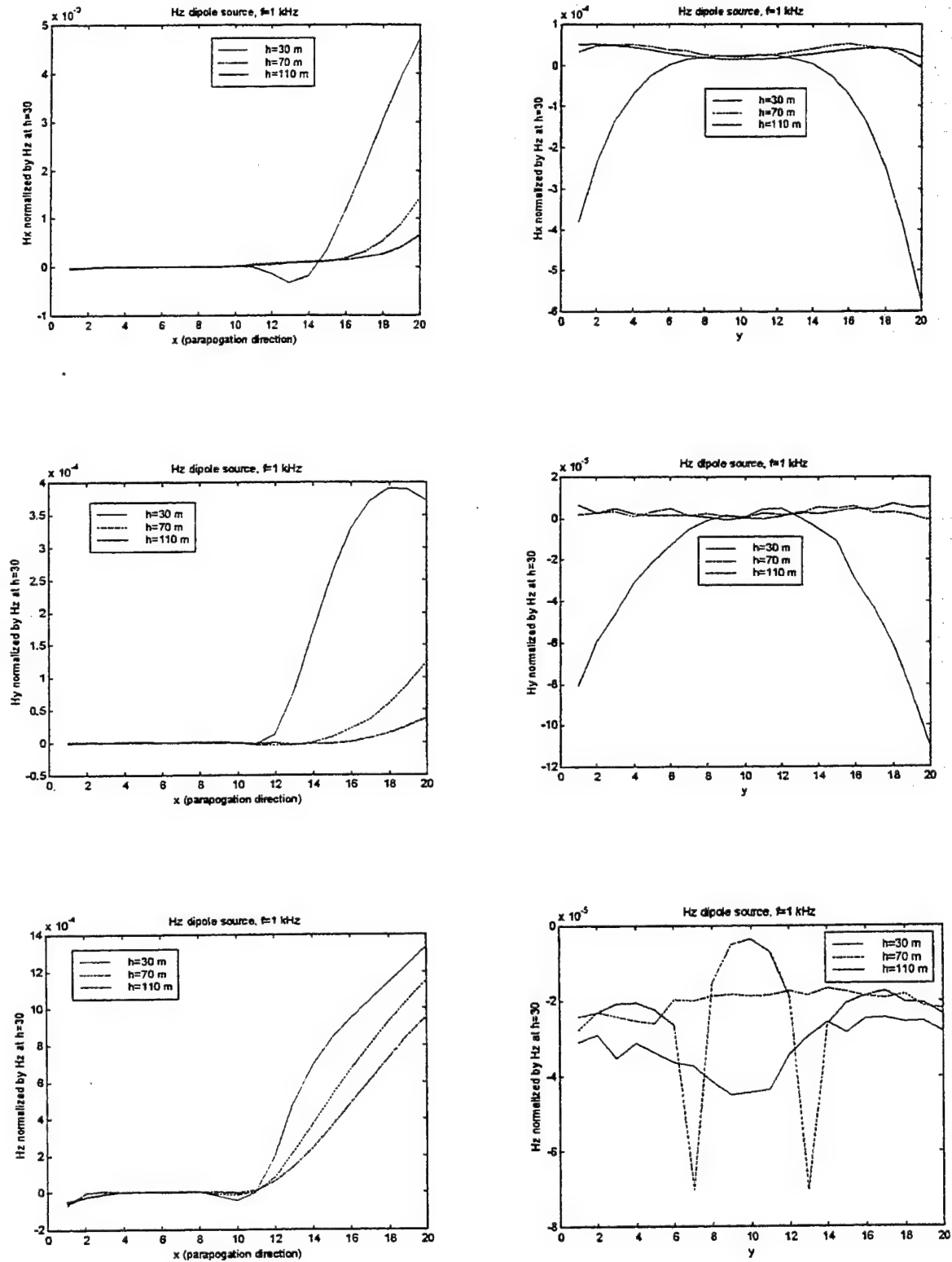Figure 2   H Field components measured at different heights (30.70 and 110 meters) as functions of x and y in meters. H fields are normalized by H_y in the absence of the bunker. (Plane Wave Excitation, 1 kHz).

Figure 3   Same as Figure 2 but for 10 kHz.

Figure 4   Same as Figure 2 but for Magnetic Dipole Source at 1 kHz (Dipole is placed 80 m to the left of the bunker, see Figures 6 and 8).

Figure 5   Same as Figure 4 but for 10 kHz.

Figure 6   Field distributions above the source; top figures dipole source; bottom figures plane wave source.

Figure 7 and 8   Two dimensional cuts for fields above the sources.

Figure 9   Plane wave excitation; Measurement points in this example are above ground.

Figure 10 Hy distribution 10m above surface for 1 kHz, 5 kHz, and 10 kHz.

Figure 11   Hz/Hx and Hz/Hy distributions 10m above surface; Note that the edges of the bunker are easily detectable for this case.

Figure 12   Plane wave excitation; Field computed inside the bunker.

Figure 13   Ez field distribution inside the bunker and near it.

Figure 14   Top two figures; Variation of scattered Ez along the y-and-z- directions inside the bunker. Different color are different frequency plots.

Figure 15   Plots shows Hx distribution at z = 1m above ground. Bunker is from 20m to 40m (its height is 20m) below ground. Gradients of Hx/ x around the edges of bunker are seen in the contour plot.

Figure 16   Hy plot also 1m above ground Gradient of Hy/ y around the bunker edges are seen from this plot.

Figure 17   Plane wave excitation at f = 10 Hz

Figure 18   Plane wave excitation at f = 100 kHz

FDTD Simulation

Example 1: Plane wave excitation.
Bunker depth = 20 m
Bunker geometry: 67.5x60x40
Bunker is located from 10 to 13 in
x and y directions in following
Pictures
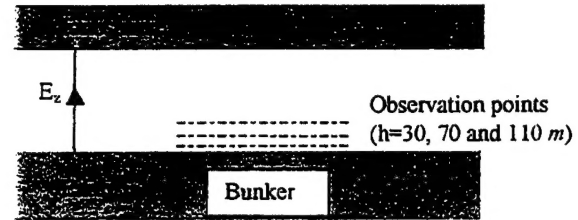
Example 2: Hz dipole source.
Bunker depth = 20 m.
Bunker geometry: 67.5x60x40.
Bunker is located from 10 to 13 in
x and y directions in following
Pitures.
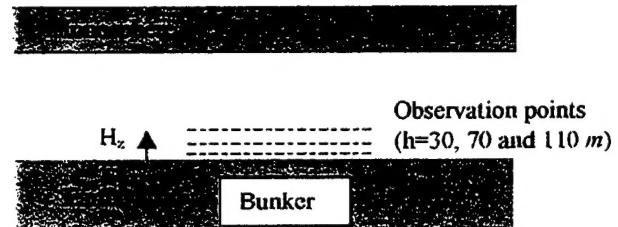
The scattered signals are obtained by calculations (incident and total fields) of two times of FDTD, which are carried out without and with bunkers, respectively. We use the Hy at 30 meters above the earth surface a the reference in example 1. Hz at 30 meters above the earth surface is used as the reference in example 2. In example 2, the Hz dipole source is located 80 meters left of the bunker.

FIGURE 1. Geometry of the bunker problem

Figure 2. H Field components measured at different heights (30.70 and 110 meters) as functions of x and y in meters. (Plane Wave Excitation, 1 kHz)

7

Figure 3. H Field components measured at different heights (30.70 and 110 meters) as functions of x and y in meters. (Plane Wave Excitation, 10 kHz)

8

Figure 4. H Field components measured at different heights (30.70 and 110 meters) as functions of x and y in meters.
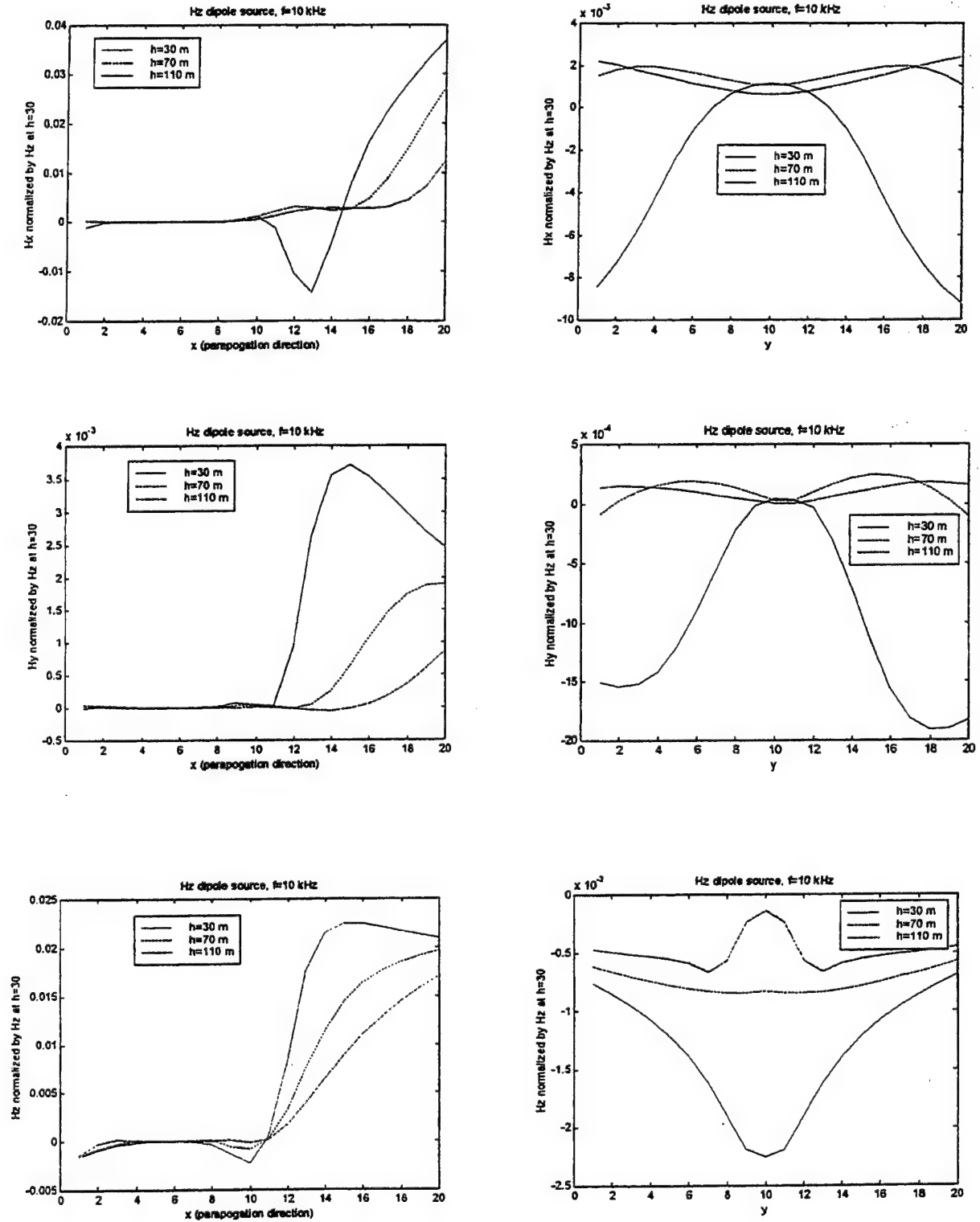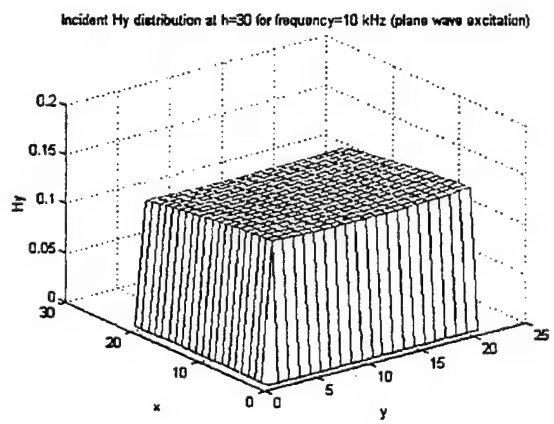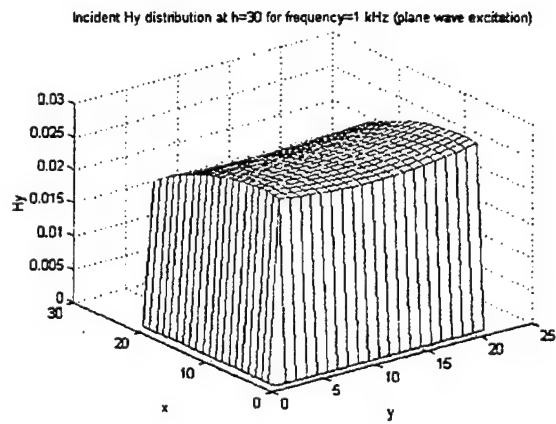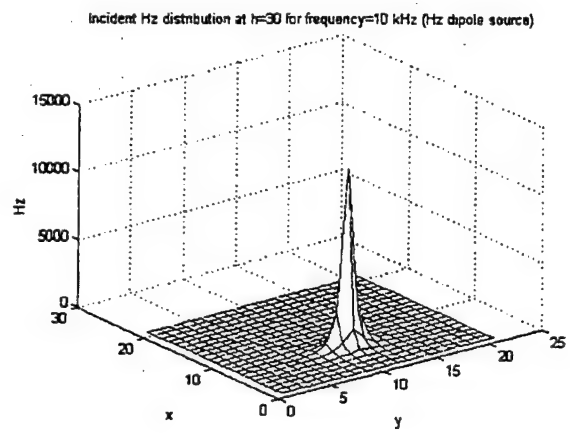(Magnetic Dipole Source at 1 kHz)

Figure 5. H Field components measured at different heights (30.70 and 110 meters) as functions of x and y in meters. (Magnetic Dipole Source at 10 kHz)
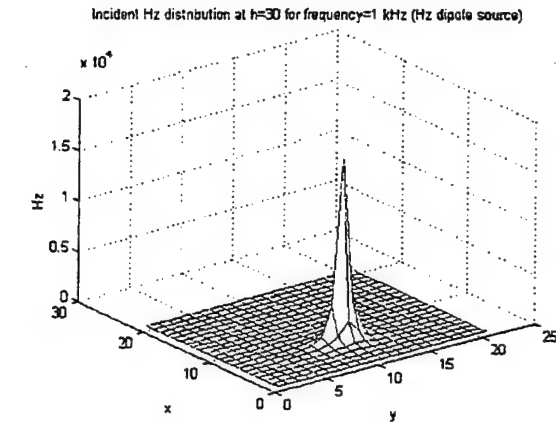
Incident Hz distribution at h=30 for frequency=1 kHz (Hz dipole source)

Incident Hz distribution at h=30 for frequency=10 kHz (Hz dipole source)

Incident Hy distribution at h=30 for frequency=1 kHz (plane wave excitation)

Incident Hy distribution at h=30 for frequency=10 kHz (plane wave excitation)

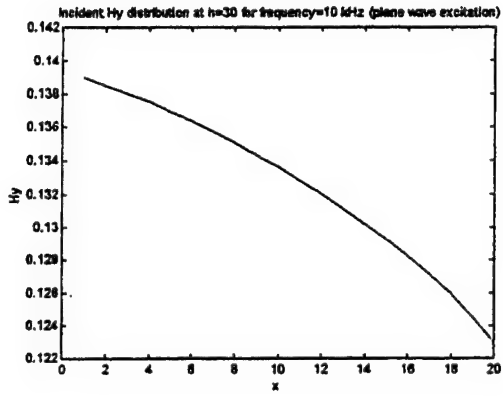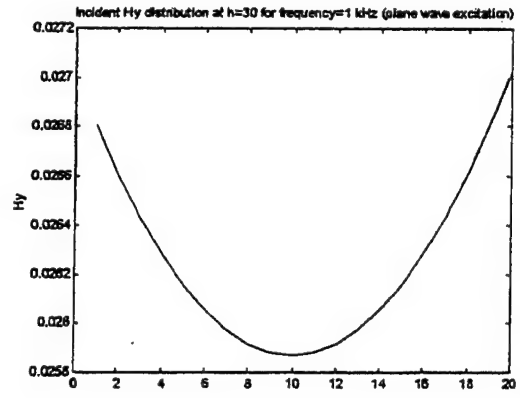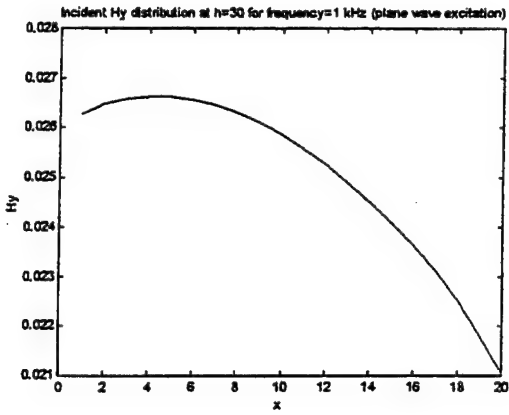Figure 6. Field distributions above the source; top figures dipole source; bottom figures plane wave source.
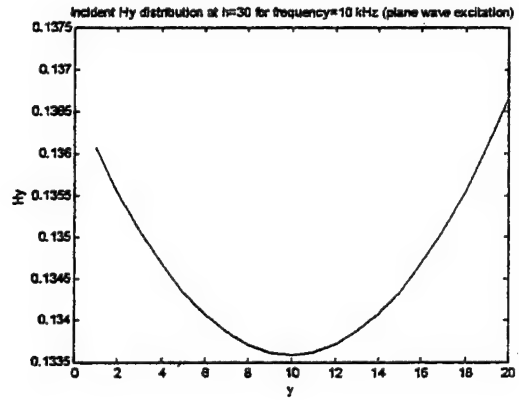
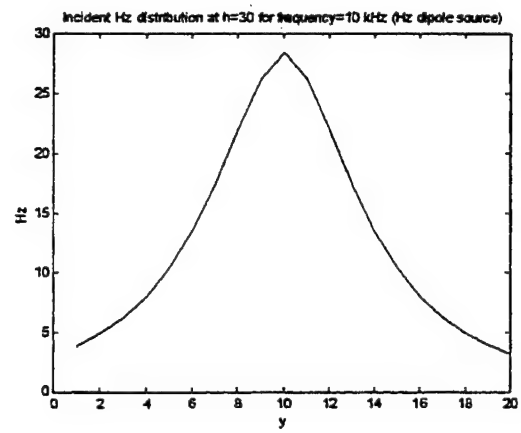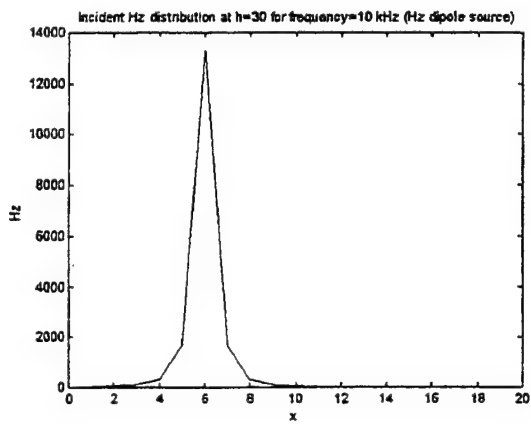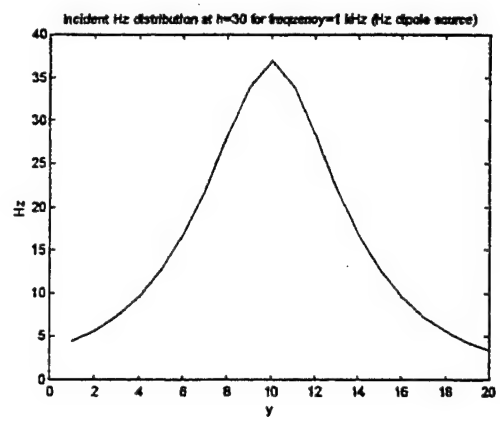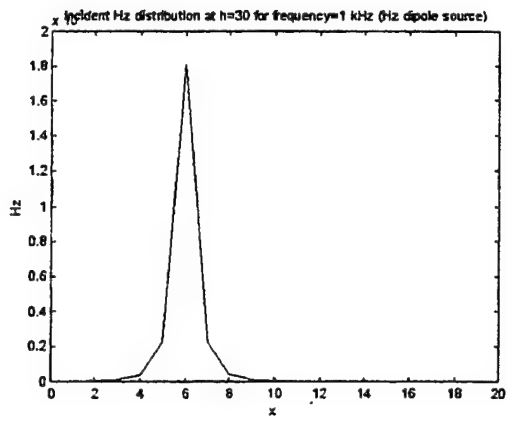Figure 7. Two dimensional cuts for fields above the sources.

Figure 8. Two dimensional cuts for fields above the sources.

13

FDTD METHOD (IMPROVED NON-UNIFORM MESH)

ABC: 6 layer-PML boundary condition;
Domain size: 120x40x120 (including PML layers) = 7757 x 800 x 10196;
Non-uniform mesh: x direction: $x_{min} = 22.5\ m$, $x_{max} = 179\ m$;
                  y direction: $y = 20\ m$;
                  z direction: $z_{min} = 20\ m$, $z_{max} = 327.9\ m$;
Earth: epsino = $2\varepsilon_o$, sigma = 0.01 m/s;
Ionosphere: epsino = $2\varepsilon_o$, sigma = 0.001 m/s;

We calculate the electric field distributions at 50 sampled frequencies from 1 kHz to 10 kHz.

Figure 9. The observation points are located 20 meters high above the earth surface. Bunker geometry:
Lx x Ly x Lz = 22.5m x 20m x 20 m.
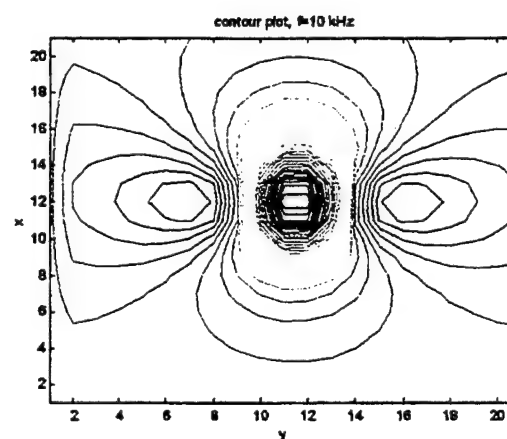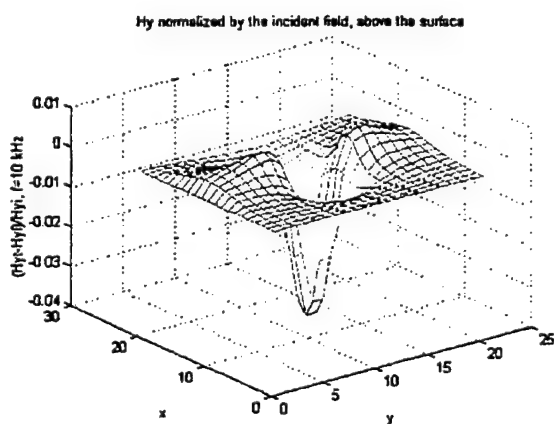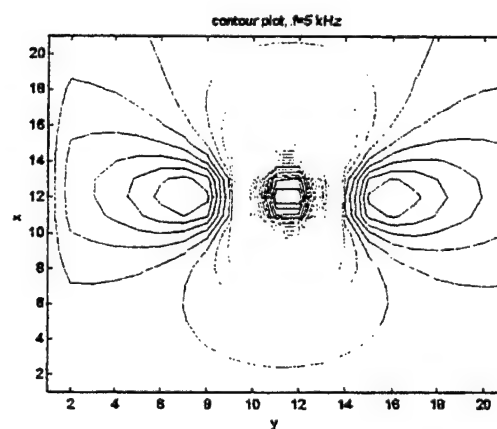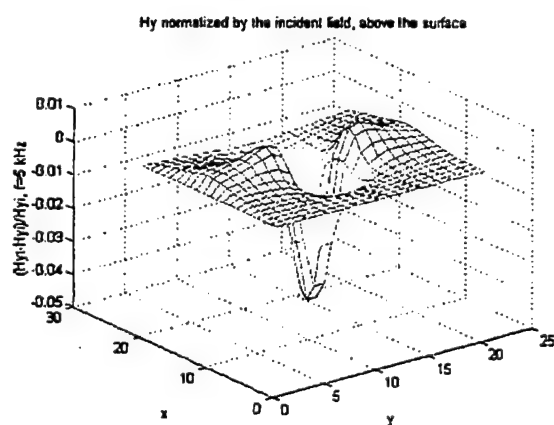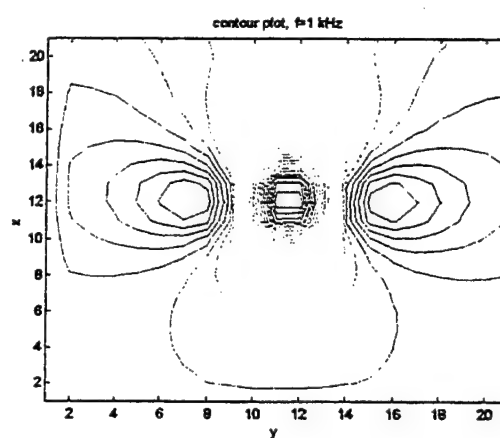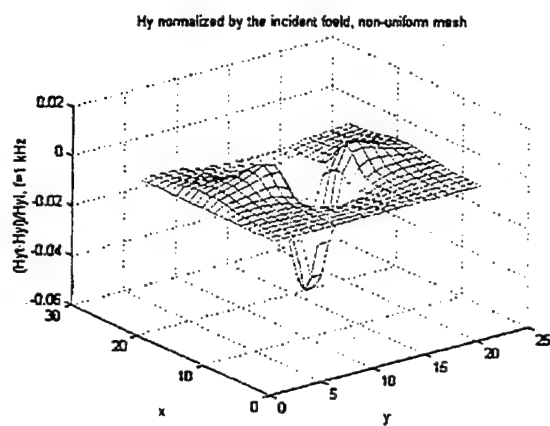
Figure 10. *Hy* distribution 10m above surface for 1 kHz, 5 kHz, and 10 kHz.
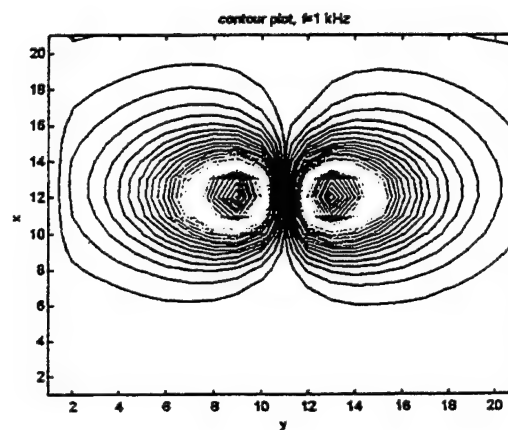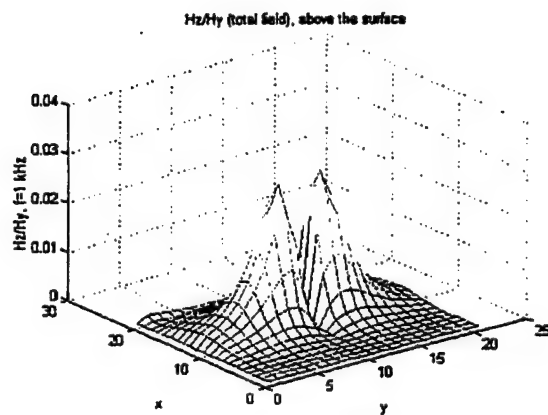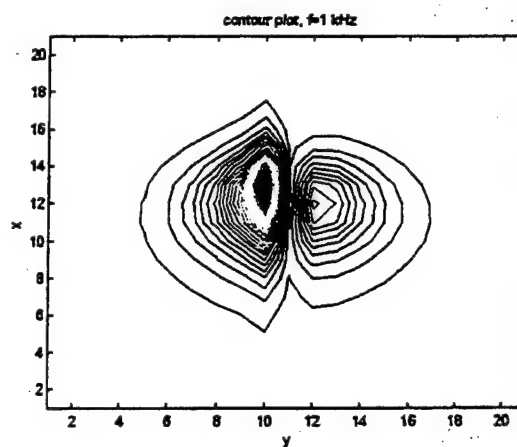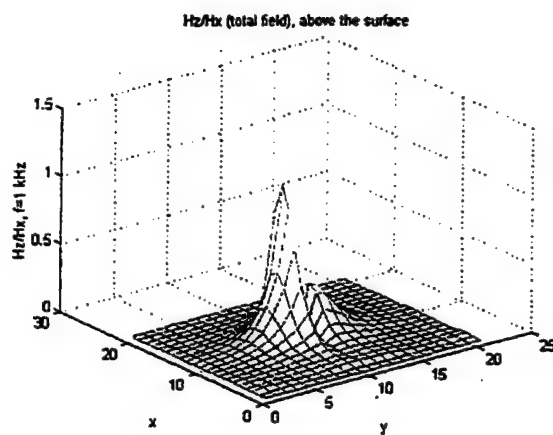
Figure 11. Hz/Hx and Hz/Hy distributions 10m above surface

FDTD METHOD (IMPROVED NON-UNIFORM MESH)

ABC: 6 layer-PML boundary condition;
Domain size: 120x40x120 (including PML layers) = 7757 x 800 x 10196;
Non-uniform mesh: x direction: $x_{min} = 22.5$ m, $x_{max} = 179$ m;
                    y direction: $y = 20$ m;
                    z direction: $z_{min} = 20$ m, $z_{max} = 327.9$ m;
Earth: epsino = $2\varepsilon_o$, sigma = 0.01 m/s;
Ionosphere: epsino = $2\varepsilon_o$, sigma = 0.001 m/s;

We calculate the electric field distributions at 50 sampled frequencies from 1 kHz to 10 kHz.

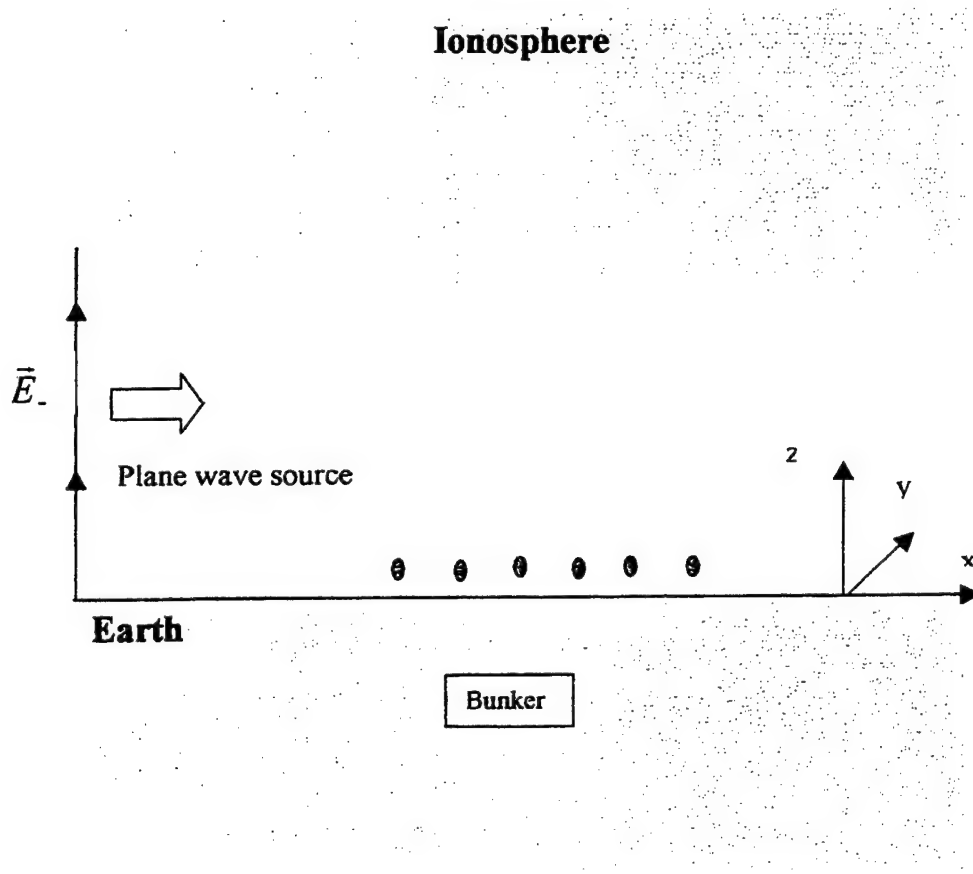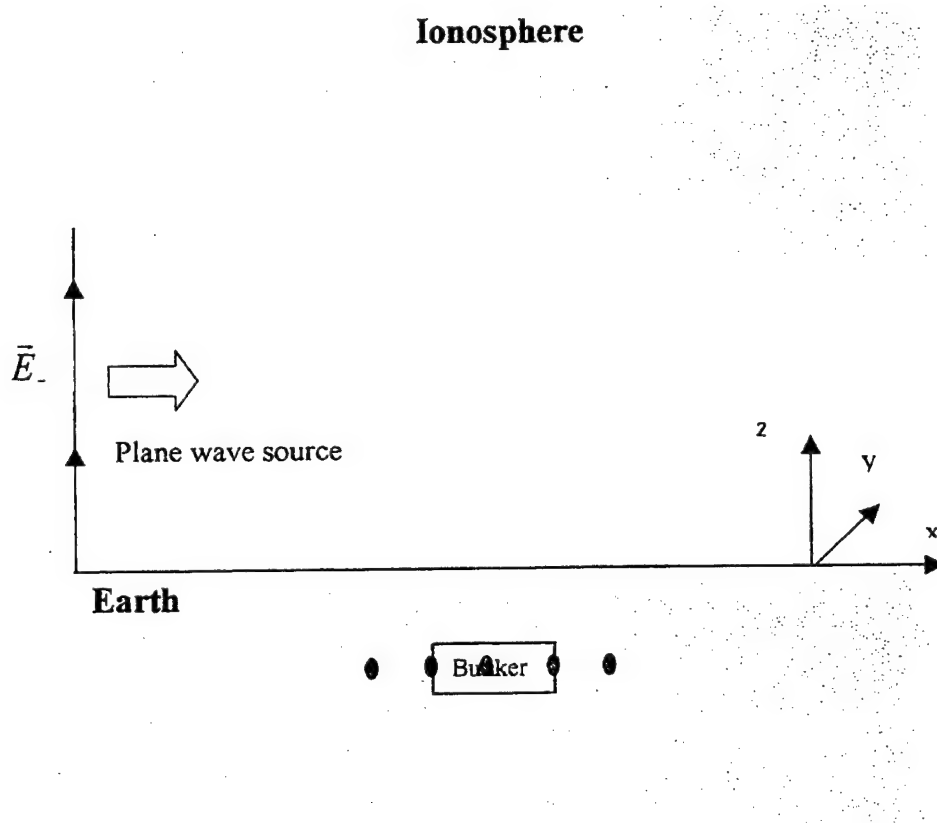Figure 12. Plane wave excitation

FDTD METHOD (IMPROVED NON-UNIFORM MESH)

ABC: 6 layer-PML boundary condition;
Domain size: 120x40x120 (including PML layers) = 7757 x 800 x 10196;
Non-uniform mesh: x direction: $x_{min} = 22.5\ m$, $x_{max} = 179\ m$;
                    y direction: $y = 20\ m$;
                    z direction: $z_{min} = 20\ m$, $z_{max} = 327.9\ m$;
Earth: epsino = $2\varepsilon_o$, sigma = 0.01 m/s;
Ionosphere: epsino = $2\varepsilon_o$, sigma = 0.001 m/s;

We calculate the electric field distributions at 50 sampled frequencies from 1 kHz to 10 kHz.

(1) Frequency = 1 kHz, Lx = 22.5 m, Ly = 20 m, Lz = 20 m, Depth = 40 m.
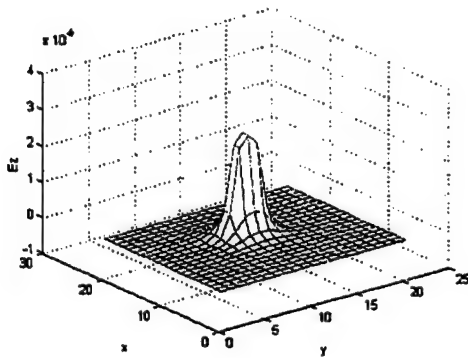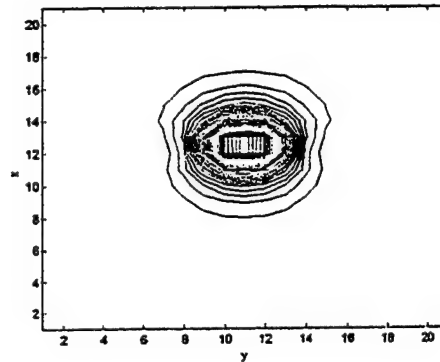
Electric field distribution on the   Contour plot of electric field on
bunker cross-section   the bunker cross-section

(2) Frequency = 10 kHz, Lx = 22.5m, Ly = 20m, Lz = 20 m, Depth = 40 m.
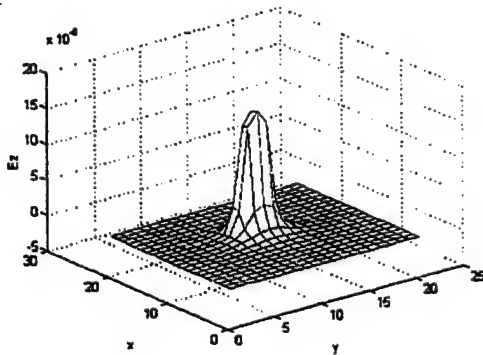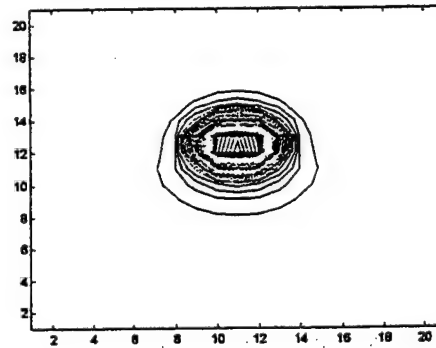
Electric field distribution on the   Contour plot of electric field on
bunker cross-section   the bunker cross-section

Figure 13. Ez field distribution inside the bunker and near it.
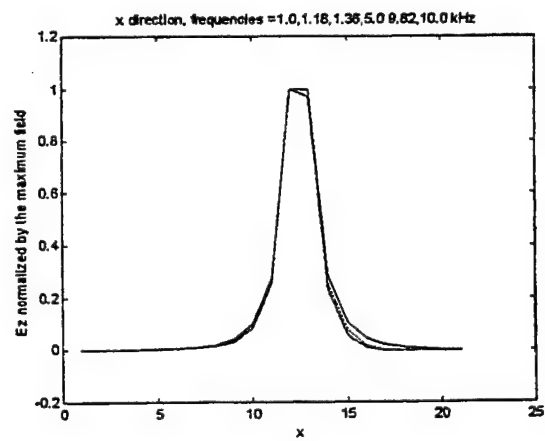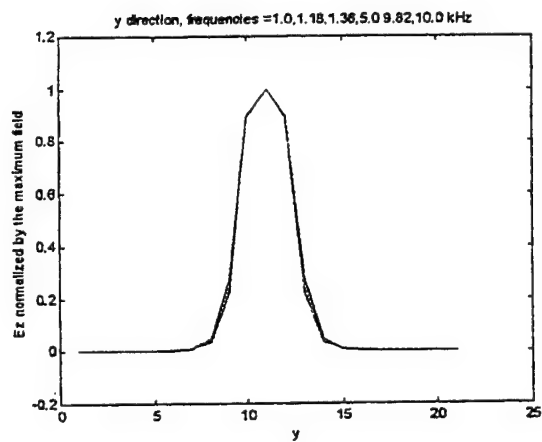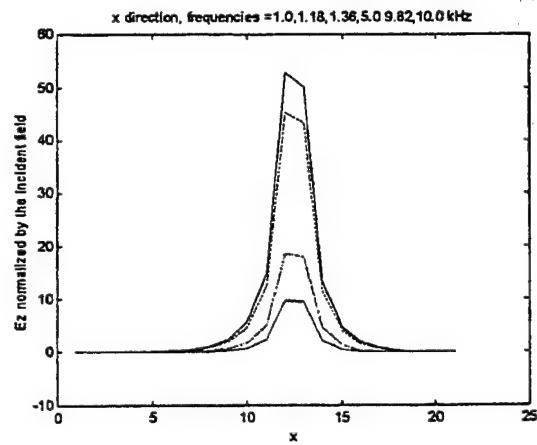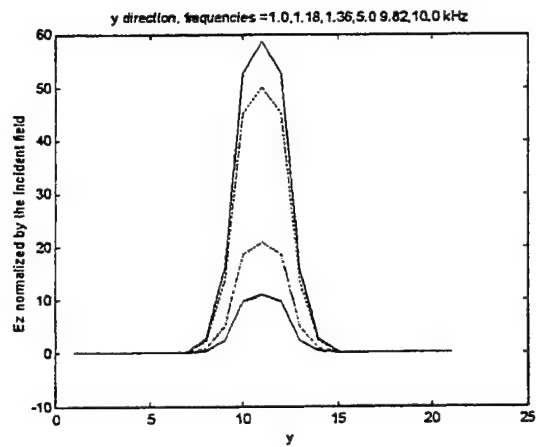
Figure 14. Variation of scattered Ez along the y-and-z- directions inside the bunker.

Legend (top plot):
- 0.0082 — 0.0090
- 0.0075 — 0.0082
- 0.0067 — 0.0075
- 0.0060 — 0.0067
- 0.0052 — 0.0060
- 0.0045 — 0.0052
- 0.0037 — 0.0045
- 0.00300 — 0.0037
- 0.00225 — 0.00300
- 0.00150 — 0.00225
- 7.5E-4 — 0.00150
- 0 — 7.5E-4

xyz_prim=0 0 -40 z_prm1_2=-40 -20 z=1
lambda=3e+08 k0=2.0944e-08 frequency=1
eps1=4 sigma1=0.001
k1=6.2832e-05+i*-6.2832e-05
eps2=1 sigma2=0.0001
x1_x2=100 180 y1_y2=100 120
k2=1.98692e-05+i*-1.98692e-05
n=11 points=2048
point2=4096 mult=8388608
xstep=3.125 ystep=3.125

Legend (bottom plot):
- 0.917 — 1.00
- 0.833 — 0.917
- 0.750 — 0.833
- 0.667 — 0.750
- 0.583 — 0.667
- 0.500 — 0.583
- 0.417 — 0.500
- 0.333 — 0.417
- 0.250 — 0.333
- 0.167 — 0.250
- 0.083 — 0.167
- 0 — 0.083

Figure 15. Plots shows Hx distribution at z = 1m above ground.

$$|H_x| \text{ in } \frac{A}{m}$$

$x_1 = 100$ m
$x_2 = 180$ m
$y_1 = 100$ m
$y_2 = 120$ m
$z_1 = -40$ m
$z_2 = -20$ m
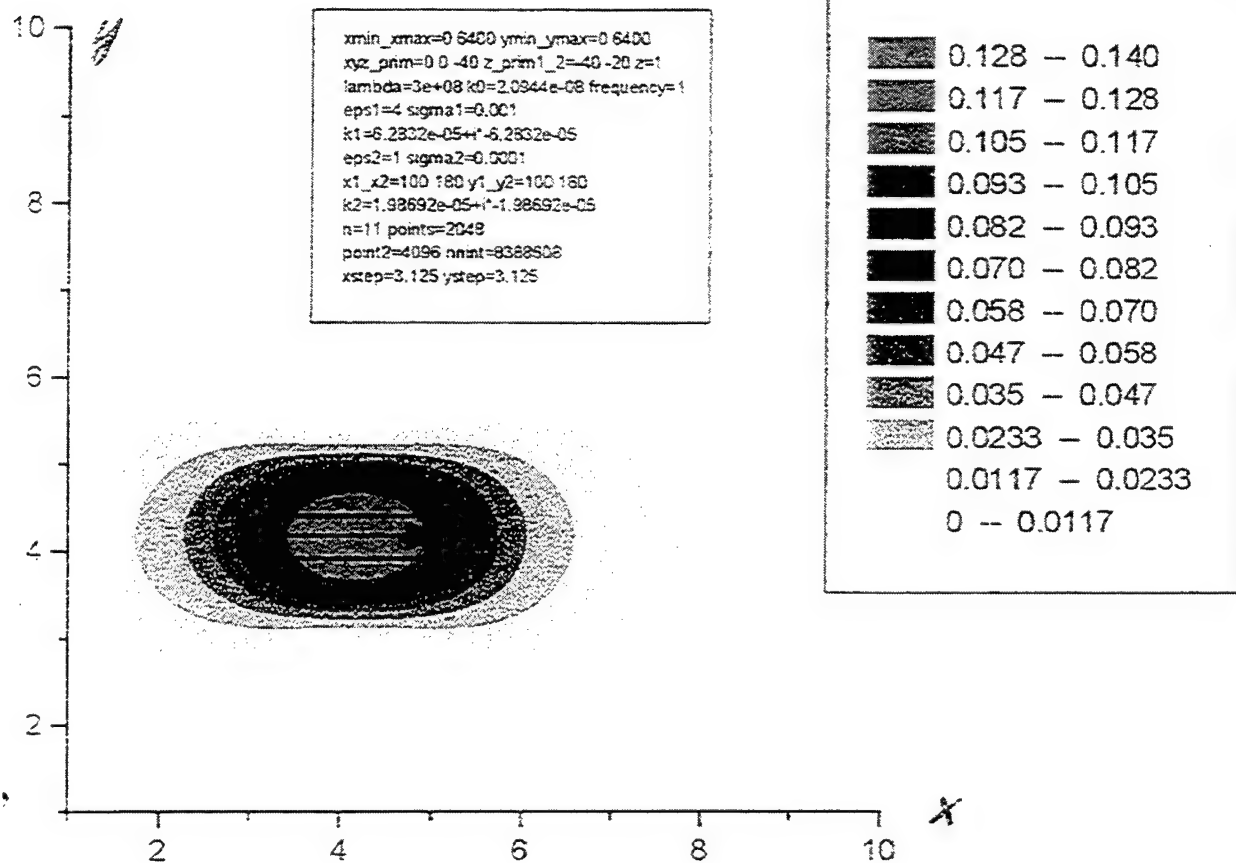
20

Figure 16. Hy plot also 1m above ground Gradient of Hy/ y around the bunker edges are seen from this plot.

$$|H_x| \text{ in } \frac{A}{m} \quad \text{at } Z = 1\text{m}$$

$x_1 = 100 \text{ m}$
$x_2 = 180 \text{ m}$
$y_1 = 100 \text{ m}$
$y_2 = 180 \text{ m}$
$z_1 = -40 \text{ m}$
$z_2 = -20 \text{ m}$

PLANE WAVE EXCITATION. F = 10Hz

Input Geometry (G5):

The parameters of the cavity are as follows:

Height	10 m
Length	30 m
Width	10 m
The cavity is located in the ground at a depth of	50 m

The parameters of the media are chosen as follows:

Dielectric permittivity of the medium above (air)	$1.0\varepsilon_0$ farad/meter
Conductivity of the medium above (air)	1.0 e-5 siemens/meter
Dielectric permittivity of the medium below (ground)	$2.0\varepsilon_0$ farad/meter
Conductivity of the medium below (ground)	1.0 e-3 siemens/meter

Angle of incidence of the plane wave : $\theta_1 = 89.99°$. Electromagnetic field is calculated at the distance of 0m above the ground.

Side view:

The level of 0 meters above the ground, where the field is calculated

Figure 17. Plane wave excitation at f = 10 Hz..

|H_z| component of the field above the ground (z=0m).

▦	1.925E-9 -- 2.2E-9
▦	1.65E-9 -- 1.925E-9
	1.375E-9 -- 1.65E-9
▦	1.1E-9 -- 1.375E-9
▦	8.25E-10 -- 1.1E-9
▦	5.5E-10 -- 8.25E-10
▦	2.75E-10 -- 5.5E-10
■	0 -- 2.75E-10

X Axis

▦	2.45E-9 -- 2.8E-9
▦	2.1E-9 -- 2.45E-9
	1.75E-9 -- 2.1E-9
▦	1.4E-9 -- 1.75E-9
▦	1.05E-9 -- 1.4E-9
▦	7E-10 -- 1.05E-9
▦	3.5E-10 -- 7E-10
■	0 -- 3.5E-10

X Axis

Figure 17. Plane wave excitation at f = 10 Hz..

|H_y| component of the field above the ground (z=0m).
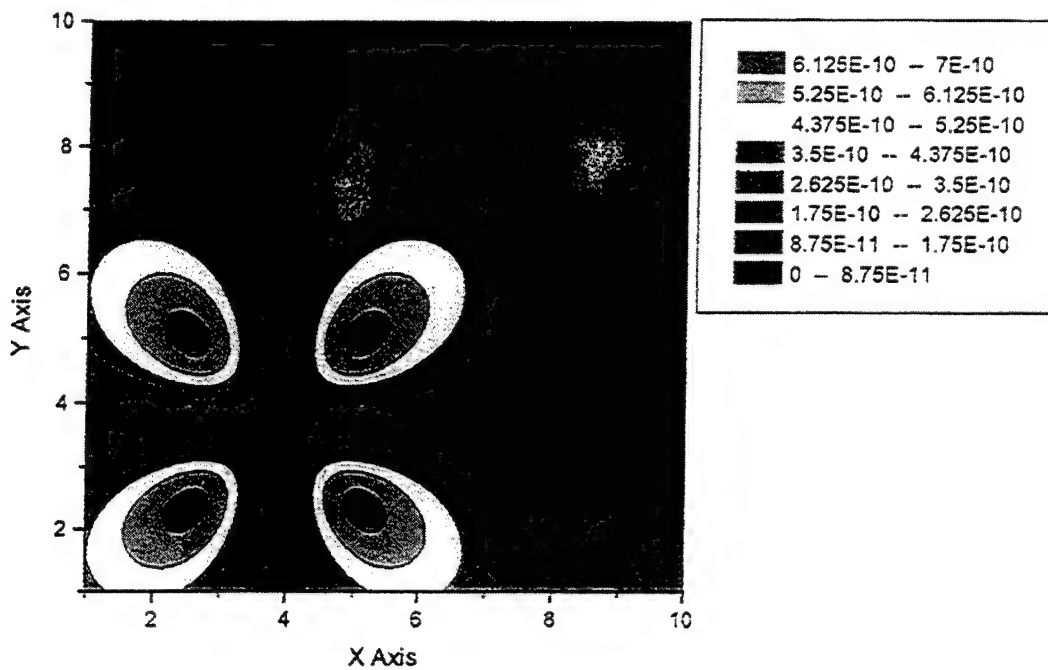
|E_y| component of the scattered filed above the ground (z = 0m).
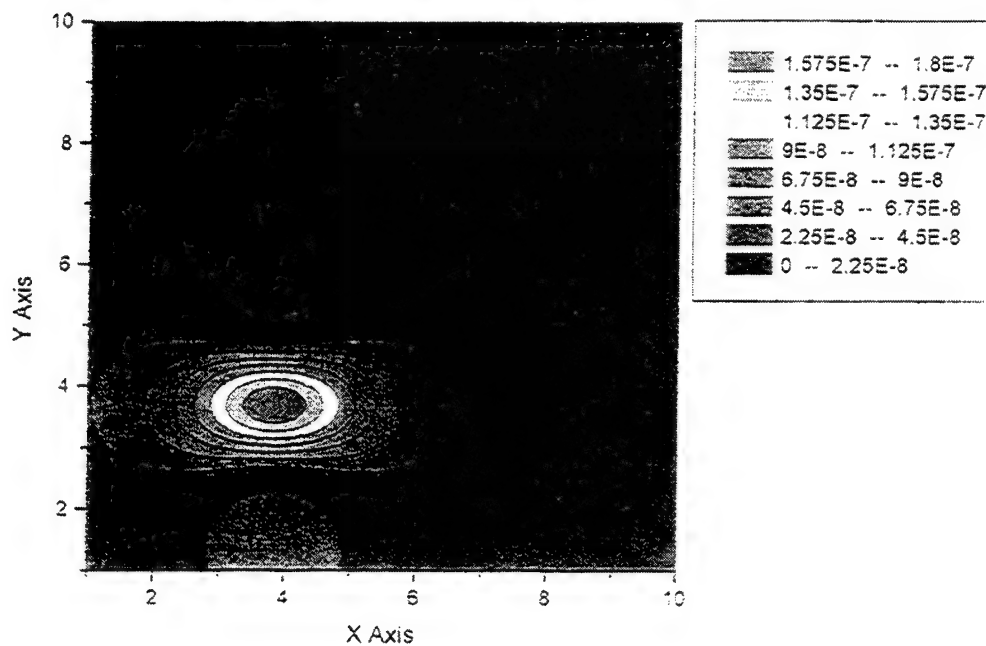
Figure 17. Plane wave excitation at f = 10 Hz..

|Ey| component of the total field above the ground (z=0m).
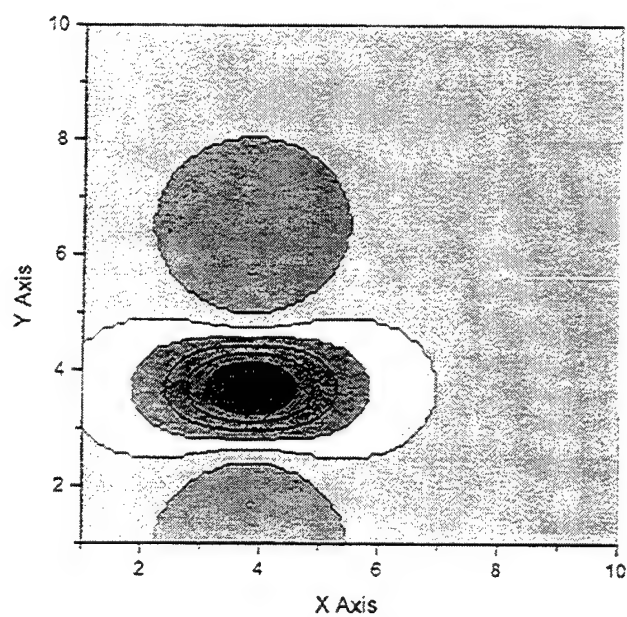
|Ex| component of the scattered field above the ground (z=0m).

4.813E-8 -- 5.5E-8
4.125E-8 -- 4.813E-8
3.438E-8 -- 4.125E-8
2.75E-8 -- 3.438E-8
2.063E-8 -- 2.75E-8
1.375E-8 -- 2.063E-8
6.875E-9 -- 1.375E-8
0 -- 6.875E-9
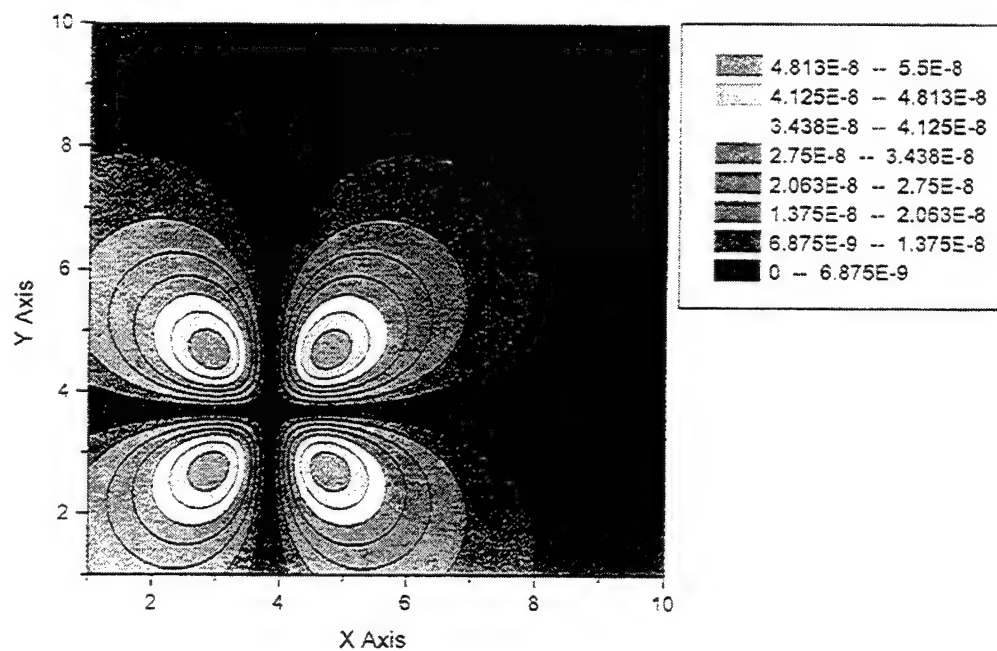
Figure 17. Plane wave excitation at f = 10 Hz..

Z=|Ey/Hx| at the interface z=0m.
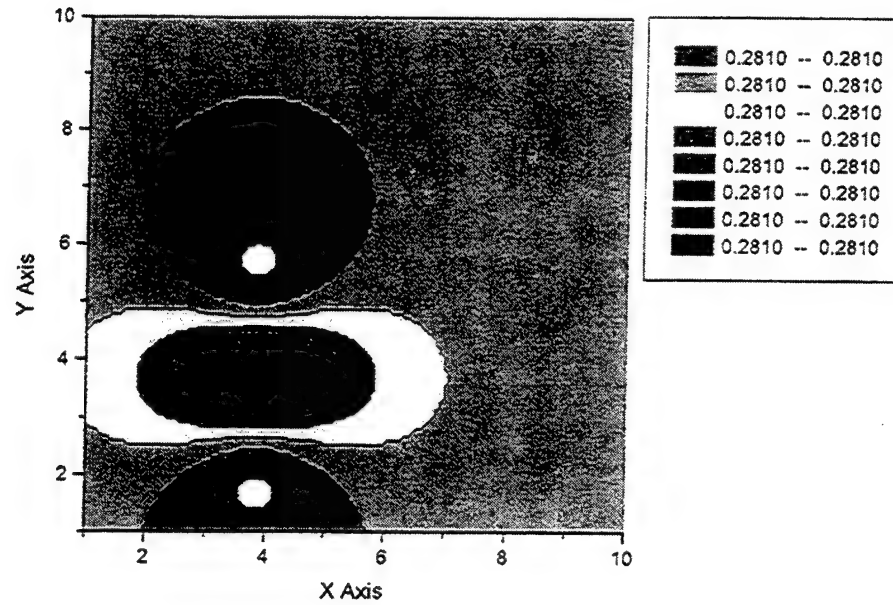
Z=|Hz/Hx| at the interface z=0m.

Figure 17. Plane wave excitation at f = 10 Hz..

26
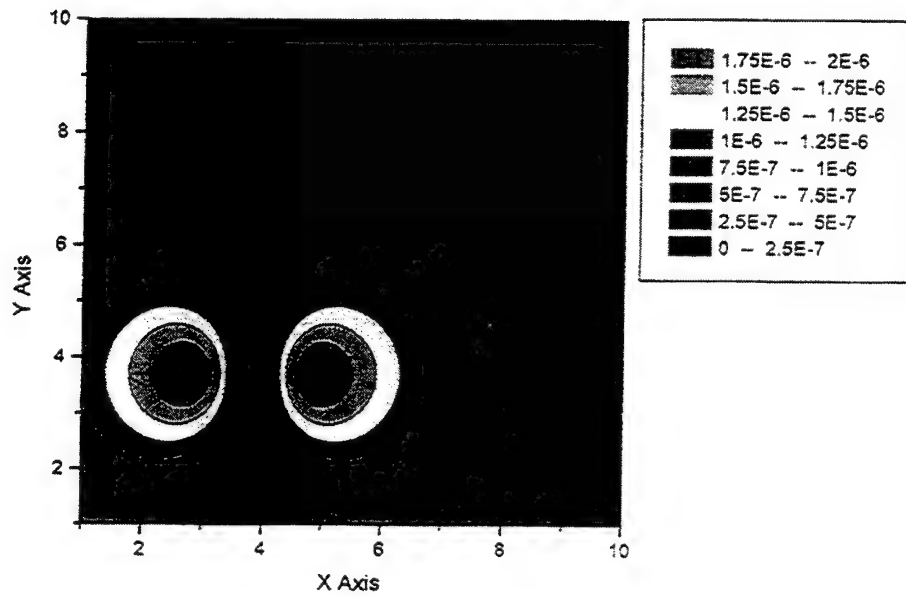
PLANE WAVE EXCITATION. F = 100 000Hz

Input Geometry (G5):

The parameters of the cavity are as follows:

Height	10 m
Length	30 m
Width	10 m
The cavity is located in the ground at a depth of	50 m

The parameters of the media are chosen as follows:

Dielectric permittivity of the medium above (air)	$1.0\varepsilon_0$ farad/meter
Conductivity of the medium above (air)	1.0 e-5 siemens/meter
Dielectric permittivity of the medium below (ground)	$2.0\varepsilon_0$ farad/meter
Conductivity of the medium below (ground)	1.0 e-3 siemens/meter

Angle of incidence of the plane wave : $\theta_1 = 89.99°$. Electromagnetic field is calculated at the distance of 0m above the ground.

Side view:

The level of 0 meters above the ground, where the field is calculated

Figure 18. Plane wave excitation at f = 100 kHz

27

$|H_z|$ component of the field above the ground (z=0m).

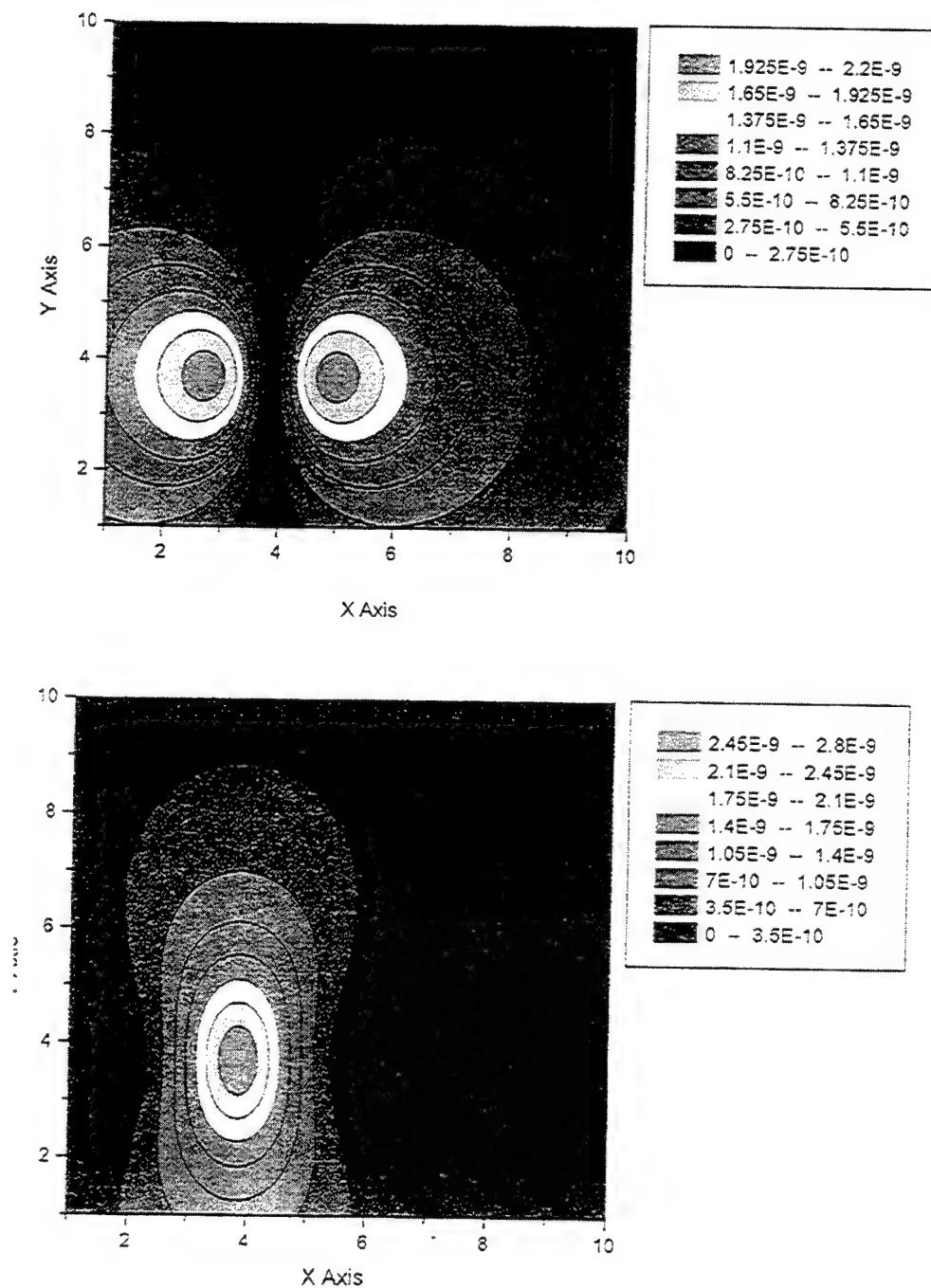## $|H_x|$ component of the scattered field above the ground (z=0m).

Figure 18. Plane wave excitation at f = 100 kHz

28

|H_y| component of the field above the ground (z=0m).
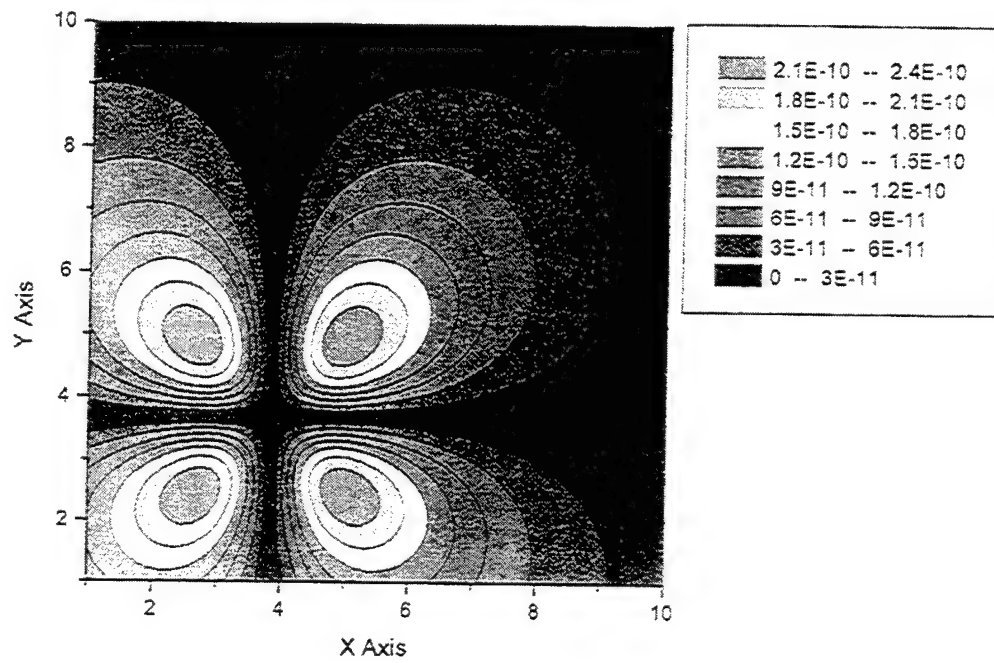
|E_y| component of the scattered field above the ground (z=0m).
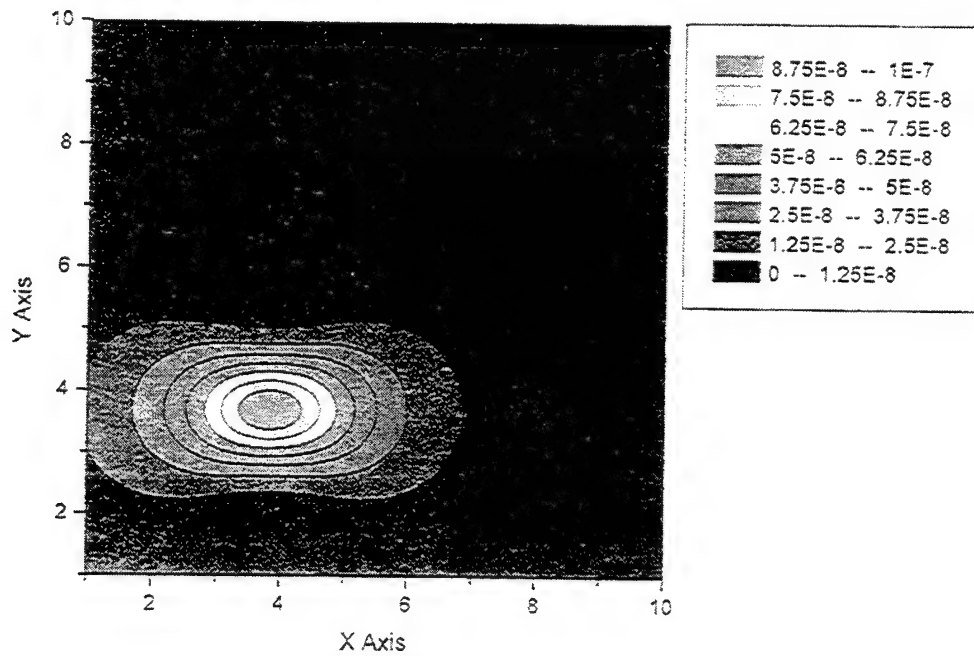
Figure 18. Plane wave excitation at f = 100 kHz

|Ey| component of the total field above the ground (z=0m).
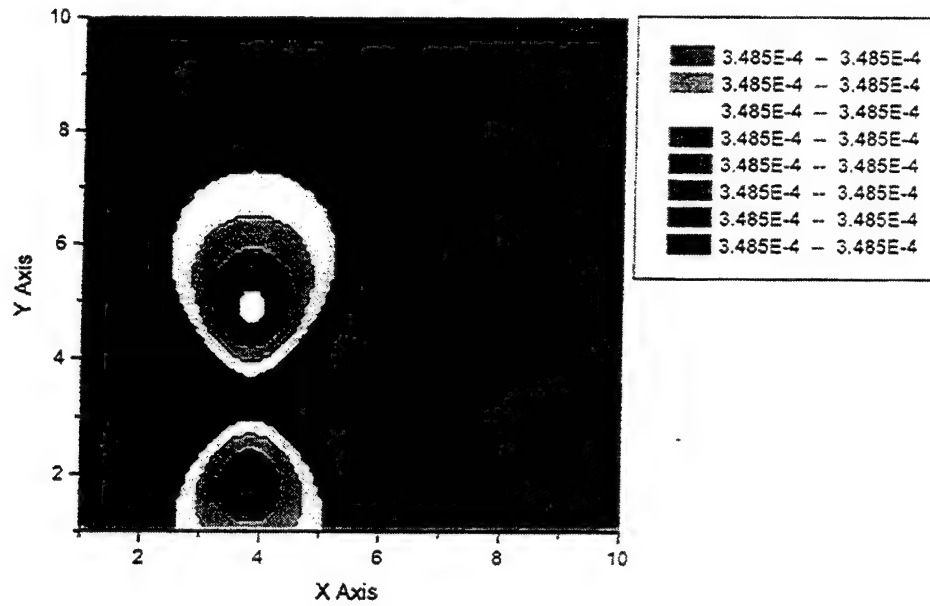
▣	3.485E-4 – 3.485E-4
▨	3.485E-4 – 3.485E-4
	3.485E-4 – 3.485E-4
■	3.485E-4 – 3.485E-4
■	3.485E-4 – 3.485E-4
■	3.485E-4 – 3.485E-4
■	3.485E-4 – 3.485E-4
■	3.485E-4 – 3.485E-4

|Ex| component of the scattered field above the ground (z=0m).

▣	1.925E-8 – 2.2E-8
▨	1.65E-8 – 1.925E-8
	1.375E-8 – 1.65E-8
■	1.1E-8 – 1.375E-8
■	8.25E-9 – 1.1E-8
■	5.5E-9 – 8.25E-9
■	2.75E-9 – 5.5E-9
■	0 – 2.75E-9

Figure 18. Plane wave excitation at f = 100 kHz

Z=|Ey/Hx| at the interface z=0m.

28.0986 max
28.0969 min
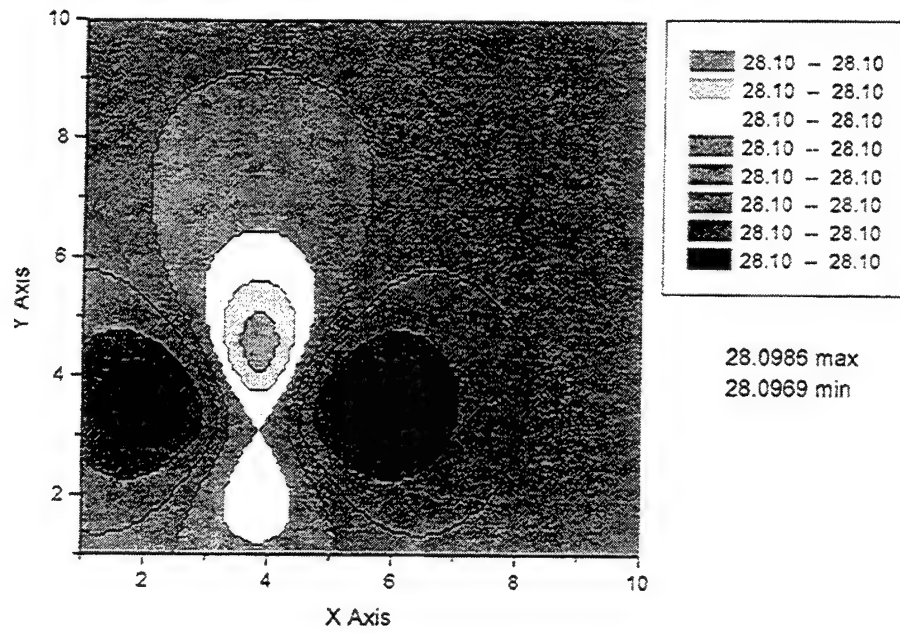
Z=|Hz/Hx| at the interface z=0m.

Figure 18. Plane wave excitation at f = 100 kHz

31

3. CONCLUSION

A novel 3-D E.M. model has been developed. This allows modeling of the E.M. field components at any location, inside the ground, inside the tunnel, above the ground, etc. to be determined. The ground can be modeled in 3-D using inhomogeneous material and any arbitrary shaped tunnel, cavity, void or anomaly can be modeled. The tunnel or cavity may be a void or can be filled with dielectric and conductive material (water, metal rods, pipes, electric cables, etc.).

Various E.M sources can be used for excitation. The sources can be placed far away, resulting in a wave propagating in the earth-ionosphere waveguide above the region of interest. This situation is similar to what would be expected for HAARP or from other ELF/VLF sources. Otherwise, the E.M. sources can be located in nearby ground using magnetic field (magnetic loop) or electric field excitation (electric dipole). The sources can be placed above the ground or can be embedded in the ground. Sources may also be placed in the cavity itself (generators, power cables etc. in the tunnel).

The frequency of excitation can be varied from d.c. to arbitrarily high frequencies (MHz). A special technique has been developed to extend the low frequency limit and still maintain computational accuracy. There is no previously existing code that allows such generalized treatment of the forward problem.

Limited simulations have been performed during the study to estimate the feasibility of remote sensing using electromagnetic techniques. Both the ground level field and the field above the ground have been estimated and the detactability of various tunnels at different depths and of different sizes has been established.

This simulations have established that the complex field interactions demand 3-D modeling and the result may not be extrapolated from 2-D models or by using simpler geometries. Results of the 3-D modeling are essential before solving the inverse problems.

Results of preliminary simulations are extremely encouraging. The field perturbations in various components contain enough signatures of the underground structures. The field perturbations of major components are easily detectable using sensitive sensors. Both plane wave and localized sources can be used for optimized detection depending on soil conditions, depth, tunnel geometry and orientation and most significantly on the sensor deployment scenario. The generalized E.M. code can be used for the optimization and for development of inversion procedure.

Field measurements can be performed either at the ground level or using aerial vehicles. Underground (using boreholes) sensors may also be modeled and considered. The practical frequency range varies from a few Hz to hundreds of kHz. Various sources of excitation and methods of sensor deployment can be used for optimized detection of various underground structures.

For low frequencies (i.e. d.c. to kHz) magnetic field sensors are practical. There are basically two types of magnetic field sensors, magnetometers and induction coils. We have surveyed the complete range of technology and two types of magnetometers 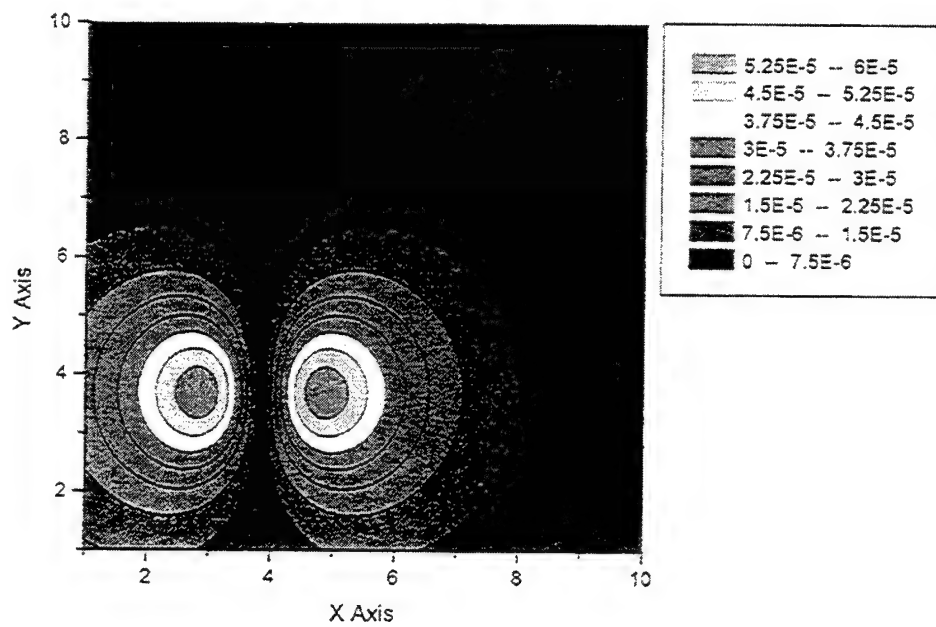seem promising. One is fluxgate magnetometer and the other is Atomic Resonance magnetometer. These magnetometers offer magnetic field measurements from d.c. to tens of Hz. The frequency range for specially designed fluxgate magnetometers can be extended to tens of kHz. Design for such an extension in frequency range has been performed.

Induction coils on the other hand provides measurements of dB/dt and offer the most sensitivity for frequencies above a few Hz. For low frequency operation (at tens of Hz), the induction coils are extremely bulky. An induction coil with high sensitivity (10^{-9} Gauss $Hz^{-1/2}$ at 1 Hz) typically has dimension of 1m x 10cm x 10cm and eights about 15 pounds. If the low frequency limit is extended to say a few kHz, the size and weight become comparable to that of fluxgate magnetometer.

Fluxgate magnetometers currently offer sensitivity of about 5×10^{-8} $GHz^{-1/2}$ at 1 Hs. They operate from d.c. to some tens of Hz. CRS has developed the most sensitive fluxgate magnetometers. These devices typically are contained with 2-inch cubes and weigh a few ounces. Current fluxgate devices use analog electronics. Initial design and plans for extending the frequency range have been drawn. Further improvements are needed in terms of improving the electronics (using digital) and in improved core materials.

32

Orthogonality of theses sensors (both fluxgate and induction coils) are also extremely important, particularly for UAV based applications. Vibration and rotational effects in the UAV based applications can be minimized using three orthogonal components and by forming the scalar value. Further improvements in orthogonality are needed. Combinations of fluxgate and induction coil sensors provide wide frequency coverage.

Atomic magnetometers directly offer the scalar value of the magnetic field and may be useful for UAV based applications. Currently they offer sensitivities of the order of 10^{-7} GHz at 1Hz. Further development of this technology offers strong promise of attaining sensitivities comparable to fluxgate magnetometers. Total field measurements, however, may not provide the necessary sensitivity for E.M sensing.

Plans for experiments using both fluxgate and induction coil sensors (available at CRS) have been made. A versatile system complete with sensors, data-acquisition and analysis has been designed and plans for experiments at HAARP have been made.

3. BIBLIOGRAPHY

Allen, G.I., 1995 Unique Man Portable Five Element Fluxgate Gradiometer Systems., SPIE Conference Proceedings, 2496; Detection Technology for Mines and Mine like Targets, pp. 384.

Clem, T.R. 1995 Superconducting Magnetic Sensors for Mine Detection and Classification, SPIE Conference Proc., 2496; Detection Technology for Mines and Mine Like Targets, pp. 374

DeProspo, D. and R. DiMarco Detection and Discrimination Techniques for Total Field Magnetometers and Multi-Axis Gradiometers, Final Report by ARETE Engineering Technology, SFIM-AEC-ET-CR 95093.

Ganguly, S. 1996 Generation of VLF/ELF Waves using Ionospheric Nonlinearity, Nature, 320, 6062.

Ganguly, S. 1987 Magnetometer for Detecting Metallic Objects in Earth's Magnetic Field, U.S. Patent 4675606.

Ganguly, S. 1998 Magnetic Array, Final Report, DARPA(DAAH01-87-C-0986).

Ganguly, S. 1996 Magnetic Array, Final Report, DAAH01-93-C-R124.

Ganguly, S., W.E. Gordon and K. Papadopoulos 1986 Active Nonlinear VLF Generation in the Ionosphere, Phys. Rev. Lett., 57, 641.

Gershenson, M., 1991 High Temperature Superconductive Flux Gate Magnetometer, IEEE Trans. On Magnetics, 27, 3055.

Wynn et al., 1975 Advanced Superconducting Gradiometer Magnetometer Arrays and a Novel Signal Processing Technique, IEEE Trans. on Magn. MAG-11, pp. 701.

Wynn et al., 1995 Magnetic dipole localization using the gradient rate tensor measured by a five axis magnetic gradiometer with known velocity; SPIE Conference Proceedings 2496, Detection Technologies for Mines and Mine like Targets, pp. 357.

APPENDIX A: SENSORS

Various types of E.M. sensors have been investigated. Details of these sensors are described in the following sections. For frequencies below tens of kHz the magnetic field sensors are most promising. This is merely because of their relative compactness compared to the electric filed sensors.

Magnetic sensor technology has been thoroughly investigated. For d.c. to about a few kHz the fluxgate magnetometer is the sensor of choice. Induction coils can be used for higher frequencies. Low frequency induction coils are bulky and we have performed designs to extend the upper frequency limits of fluxgate magnetometers. In our design, the effective frequency range of fluxgate magnetometers can be extended to tens of kHz. Use of a novel flux concentrator has been proposed. This will allow development of a fluxgate magnetometer with improved noise level and with frequency of operation up to tens of kHz.

For higher frequencies improvements have been made in terms of induction coil design. Both the fluxgate and induction coils measure vector components and thus are susceptible to vibrations and alignment problems. In our design, three orthogonal components are measured and scalar components can be derived when necessary. It remains to be seen whether the scalar components alone can obtain sufficient information about the target. This will be answered through numerical simulation.

Perhaps the best sensor for obtaining scalar information alone is the optically pumped magnetometer.

Our current efforts are restricted to the fluxgate and induction coil magnetometers.

An improved Magnetometer design is needed. The improvements are needed in terms of stability, ruggedness, and superior inherent noise as well as noise cancellation. The improvements are planned through the use of different core materials, superior electronics matched to the core and, most importantly, through direct digitization of the sensor outputs. The complete digital processing will allow various signal processing technique to be adopted, resulting in superior noise cancellation. This will also allow improved stability, near perfect linearity and self-calibration. The digital system will also provide dynamic feedback to minimize the overall dynamic range requirement. The digital system will allow development of and integrated circuit for the fluxgate magnetometer. This will allow a dramatic improvement in performance and at the same time will allow mass production.

Magnetic signature of ferrous objects arise through fundamental laws of physics and cannot be easily camouflaged. Improved and highly sensitive magnetometers are needed for improving the range of detection for objects with lesser amounts of ferrous components. A major impediment to sensitive detection arises through the ambient magnetic field fluctuations arising mostly from earth's magnetosphere. The typical field fluctuations amount to several $nT/Hz^{1/2}$ at 1 Hz. The targets of interest typically are slow moving and the frequency range of interest is generally below or around 1 Hz.

A technique for combating the magnetospheric field fluctuations has been developed and patented by the Principal Investigator (US Patent 4675606). The technique essentially relies on the large correlation distance of the noise file produced by the distant magnetosphere. Using multiple sensors, the noise field can be adaptively cancelled out. The technique has been further enhanced and the cancellation scheme has been extended in the frequency domain using wavelet transform. Improved signal processing allows detection of magnetic signatures well below the limit set by the ambient noise fields. One could thus utilize improved electronics to obtain superior sensors.

Analog fluxgate sensors have been developed by us with sensitivities of $5pT/Hz^{1/2}$ at 1Hz (see TableA1). These are the most sensitive fluxgate sensors and have been designed and developed at CRS. Other sensors, with sensitivities within a factor of two to five below the CRS sensors have also been available. All the fluxgate sensors utilize analog electronics and suffer from drift, aging, power supply fluctuations, large size, nonlinearity, etc. The limit in sensitivity is also set partially by analog electronics (and partially by the core material).

We propose to implement all digital electronics and investigate the possible improvements using superior core materials. All digital electronics will perform A/D conversion as close to the sensor coil as possible. Once digitalized, the processing can be performed using DSP. We proposed to use Analog

37

Devices AD 2106X DSP operating at 80 MFLOPS (see Figure A1). This arrangement will eliminate all the problems associated with analog electronics and would allow us to concentrate on the possible improvements in core material.

Noise in the core material arises mostly through Barkhausen effect, i.e., spontaneous change in domain. Various core materials can be tested for improved noise performance. Some promising candidates include: Metglass, Thin Films, and High Temperature Superconductors. Configuration of the core and the drive mechanism can also be optimized to minimize the noise.

A basic fluxgate magnetometer responds to one of the vector components of the magnetic field. Vibrations and orientation issues associated with the sensors are extremely difficult to tackle. Minute vibration in the presence of the strong earth's field can produce enough magnetic noise. A rotation of only a few arc-seconds could provide field fluctuations of the order of a pT.

Configuration of three vector elements as close to orthogonality as possible is necessary. Mechanical orientations with accuracies of a few arc-seconds have been pioneered by scientists at the Danish Technical Institute. CRS is currently collaborating with them and we propose to use the technology to achieve as much orthogonality as practical, commensurate with application, cost and sensitivity issues. Further compensation will also be performed by using an electrical cancellation scheme.

Measurements and calibration of such a sensitive system are also of critical consideration. Special enclosures have been built to shield the earth's magnetic field to a reasonable extent. The shielding below 1Hz is extremely difficult and CRS has used the noise cancellation scheme using two sensors to perform effective measurements with sensitivities of the order of pT below 1Hz. This technique will be extended to perform all tests and calibration for the improved digital fluxgate magnetometers.

The two most significant issues associated with magnetic techniques are:
1.   Cancellation of ambient filed fluctuations
2.   Removal of motion induced noise.

The background noise in the d.c. to elf bands is generated by distant sources – magnetosphere, ionosphere and distant lightning discharges. Because of the large distance and due to propagation in the earth-ionosphere waveguide, these noise fields have large correlation distances. The large spatial wavelength allows various signal-processing schemes for cancellation of the ambient field perturbation. Center for Remote Sensing has developed several such schemes. The signal processing techniques involve: correlation, digital filtering, adaptive LMS, wavelet transform and nonlinear predictive schemes. A flexible real-time system for data acquisition and analysis has been developed.

We have also developed the most sensitive fluxgate magnetometers and the complete suite of data acquisition and analysis system. The fluxgate magnetometers are extremely lightweight and provide the highest sensitivity (10^{-8} Gauss). Details of these sensors are described in Table A2. Using these techniques a robust detection system has been developed and during a recent demonstration we have demonstrated detection of a hand held rifle at a distance of 20 to 25 meters.

For more applications the most significant issues are described in Table 3. A comparison of the sensors listen in Table A1 with the issues described in Table A3, indicates that from the point of sensitivity, light weight, cost and compactness considerations, the following sensors appear promising:
1. Fluxgate
2. Piezo Magnetometer
3. Magneto-resistance
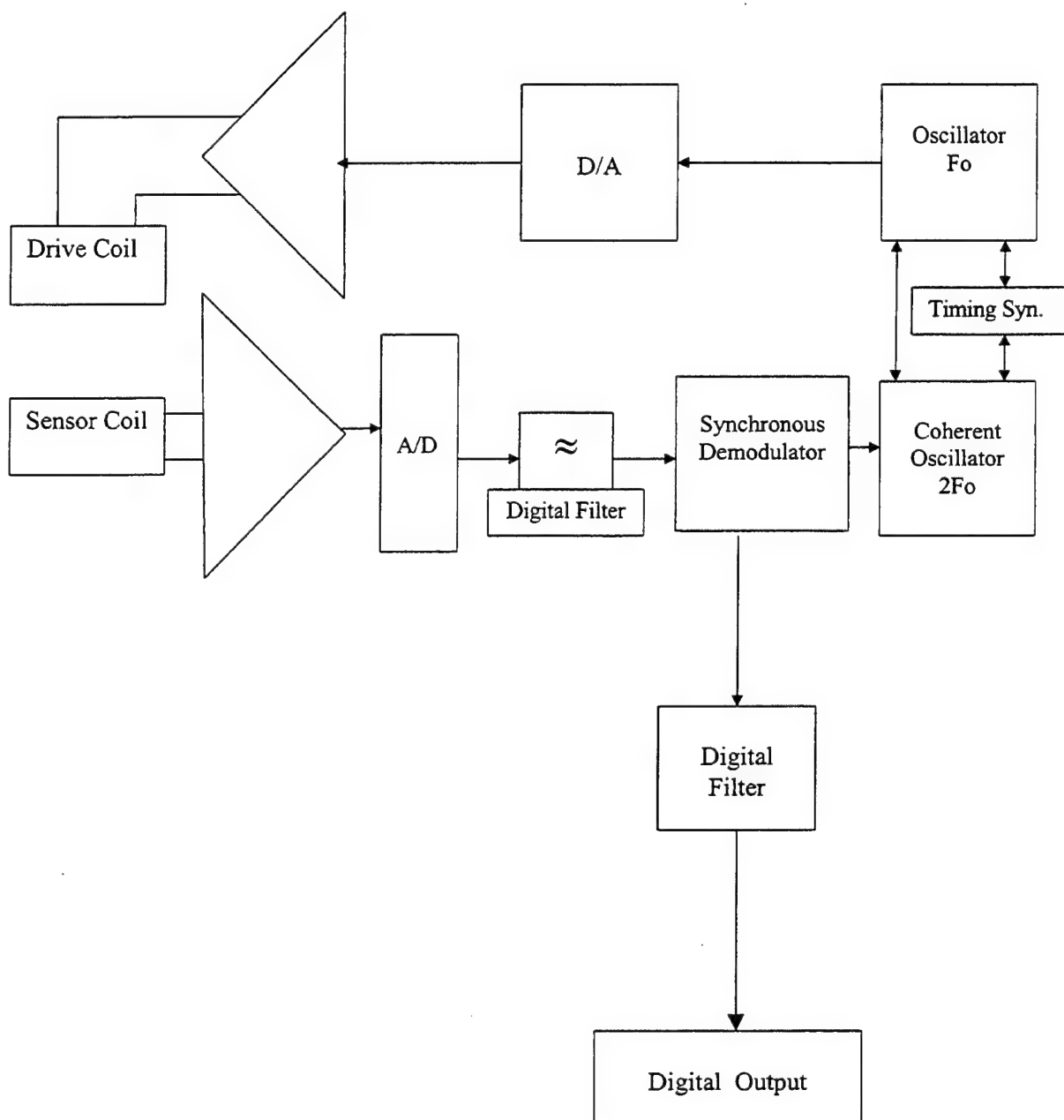4. Micro Machined Tunnel Tip
5. Laser Pumped Devices

Figure A1. Schematics for Digital Fluxgate

The fluxgate magnetometer is a developed product and is based on well-proven technology. CRS has designed and built the most sensitive fluxgate magnetometer with sensitivity on the order of 10^{-8} G/Hz$^{1/2}$ at 1 Hz. These sensors weigh a few ounces, are compact (about one cubic inch), consume little power and are ideal for embedded applications. They can be implemented either as vector magnetometers, as a gradiometer or as a scalar magnetometer by combining three orthogonal components.

Piezo magnetometers are currently under development and promise a high sensitivity of 10^{-6} G. When developed, this might offer a promising system.

Magneto-resistance can achieve 10^{-6} G. Efforts are underway at Honeywell and at Phillips (Holland) to achieve higher sensitivities. With Giant-Magneto-resistance devices, sensitivity on the order of 10^{-7} G may be achieved. When developed, these will provide the most inexpensive sensors.

Micro-machined tunnel tip was started at NRL. This promised about 10^{-6} G. Currently the effort has been abandoned.

All of these sensors are vector devices and the sensitivity to motion induced fluctuations is a major drawback for all of these devices. Perfectly aligned three axes system can be used to derive the scalar component. Perfect alignment of the three axes is a major problem. The ultimate processing error is:

$$\Delta E = H\theta^2\Omega \text{ with } \theta \approx 10^{-3} \text{ rad}, \Delta E \text{ is typically about } 10^{-10} \text{ Gauss.}$$

This requires alignment of better than 10^{-3} radians. Mismatch in electronics, shield, etc., contribute to the error. Practical systems will overall alignment accuracies of 10^{-7} Gauss have been developed.

Atomic and/or Nuclear spin resonance based techniques are fundamentally scalar devices and exhibit small motion induced effects. Laser pumped magnetometers have been developed with sensitivity on the order of 10^{-8} G. These are laboratory type systems and are extremely bulky. They are not suitable for handheld applications. There is little probability for miniaturization of these devices within a reasonable time frame.

Fluxgate magnetometers appear to be the sensor of choice at this time. We propose to develop the most appropriate magnetic sensor for embedded applications, based on our experiences with the most sensitive fluxgate systems.

Further improvements in fluxgate sensors should be directed towards the choice of superior core material and improved electronics. Various core materials available with us will be investigated.

All fluxgate magnetometers use analog circuits for amplification, filtering, phase lock loops etc. The basic magnetometer noise is limited through Barkhausen effect in the core and the analog electronics is generally adequate. Further improvements in sensitivity is possible through the incorporation of digital electronics. Most of the analog electronics can be replaced with digital electronics for filtering, phase locked loop and integrators. This will provide superior performance in terms of gain stability, output drift and dynamic range. Furthermore, this approach will lead to the development of monolithic electronics with extremely low power consumption, compact size and improved reliability.

Perhaps the most significant issue associated with magnetic sensing is the ambient fluctuations or noise. The ambient field fluctuation is typically 10^{-5} G and schemes for cancellation of these fluctuations must be provided. CRS has pioneered at technique based on large spactial coherence of these fluctuations. A patent been obtained (Magnetometers for Detecting Metallic Objects in the Earth's Magnetic Field; U.S. Patent 4675606, 1987), which uses multiple sensors for cross correlating the magnetic filed fluctuations. More recently CRS has improved the cross-correlation principle by using non-linear system prediction and adaptive filtering.

Cross correlation with multiple sensors will still be required to reduce the ambient noise. A minimum of two sensors is required from cross correlation (See Ganguly (1987)). Use of three sensors also accounts for motion induced noises. This is the principle of the gradiometer and is comprised of several (at least two) magnetometers. The data is basically differenced out through digital electronics or through a feedback field.

A gradiometer inherently cancels the environmental noise fields and responds to the small magnetic gradients established by the target. Although the sensitivity falls off as r^{-4}, instead of the r^{-3} for the total field, the end results are very similar. This is apparent from the fact that the implementation of the

gradiometer is often performed by acquiring data from several magnetometers and effectively subtracting the total field values from each other. Improved accuracies are obtained by using the tensor components instead of the total field values. The tensor components, however, are extremely sensitive to motion induced noise and will require special care. One major technical challenge involves the designing of the three vector elements in an orthogonal configuration. This allows derivation of a scalar field, which is independent of vibration and orientation. It is well established that only 5 of the 9 tensor elements (derived from 3 triaxial magnetometers) contain independent information (Wynn et. al., 1975). SQUID based gradiometers, which measure these five independent channels have been developed and the signals (time variation) have been used to invert the dipole moment and position. Sensitivities of the order of 10^{-8} Gauss have been reported using this approach. On the other hand, total field gradiometers using SQUID are reported to have attained only 3×10^{-7} Gauss (Clems, 1995).

Table A1
Status of Promising Sensors

Squid	10^{-10} G	Unchanged, No improvement expected
Induction Coil	10^{-9} G	Unchanged, No improvement expected
Fluxgate	5×10^{-8} G	Improved sensitivity attained. Some improvements can be made
Fiber Optic	10^{-7} G	NRL still trying to improve the sensitivity
Piezo Magnetometer	10^{-7} G	Podney performing experiments. Hopes to achieve 10^{-8} G.
Magnetostriction (Chip Mag)	10^{-6} G	Does not have much future.
Magneto-resistance	10^{-6} G	NO immediate improvement.
Micro Machined Tunnel Tip	10^{-6} G	Claiming to achieve up to 10^{-8} G. Doubtful
Magneto-optical	10^{-8} G	?
Laser Pumped Devices	10^{-9} G 10^{-10} G	He^3 by T.I. has lowest d.c. noise. He^4 has 1/f noise. Ce, Rb reduces gradient sensitivity

Table A2
Fluxgate Magnetometer

Extremely low noise	$< 5 \times 10^{-8} \, G \, Hz^{-1/2}$
High Sensitivity	$< 25 \, mv/nT$
Frequency Range	d.c. to kH_z
Extremely high dynamic range	$> 120 \, dB$
Extremely small, compact size	2 inch x 2 inch x 2 inch sensor
Very low power consumption	
Built – in electronics	
Digital output	
Fiber Optic Link (EMI proof)	
Interfaces to PC	

Table A3
Remote Sensor Issues

Size	Sensitivity
Ruggedness	Sensor noise, stability, calibration
Stability (acceleration, temperature)	Lower/Upper Frequency limits
Power consumption	Band pass characteristics
Portability	Dynamic range
Deployment schemes	Settling time
Configuration	Sampling rate

Analog subtraction cannot produce the desired accuracies and Digital conversion is the preferred practice (See Wynn et. al., 1995). Instead of straight differencing, various signal-processing techniques may be used to achieve superior cancellation of the so-called correlated noises. The mismatch in sensors, electronics, shields, orientation to environments, etc., all contribute to the mismatch of the correlated noises and an adaptive system performs the best. CRS has developed a nonlinear prediction based adaptive system and has demonstrated order of magnitude improvement over conventional cancellation.

A fluxgate gradiometer in which a reference sensor is used for generating the feedback field, which is applied to the other sensors has been patented and is currently being developed (Allen et. al., 1995). This approach requires careful balancing of the reference sensor and could be sensitive to environmental interferences, which produce unbalanced signals in different sensors.

Digital electronics with sufficient resolution could be used to circumvent these problems. Once the sensor outputs are digitized, they can be processed in various ways and the cancellation of the relevant events (in the temporal domain) can be undertaken using signal-processing techniques. This approach allows one to separate the events of interest form those induced by environmental noise or motion induced noise. The direct digitization also allows linearization, self-calibration and improves stability. Digital processing of signals from individual sensors allows similar analysis to be performed as those of a gradiometer. It allows various other improvements not associated with a gradiometer configuration.

One of the major difficulties, however, is to attain enough dynamic range to adequately cover the 0.5 Gauss of earth's field to 10^{-8} Gauss of the target signature. The environmental noise field is typically 10^{-5} Gauss. A d.c. (or slowly varying) bias field to reduce the effective earth's field down to the environment level can be easily attained –thus bringing the dynamics range requirement to tolerable limits. The magnitude of the bias field can be derived using signal processing techniques such as adaptive filtering (which will provide a temporal adjustment of the bias field in the presence of time varying noise and signals); wavelet or other forms of short period coherence estimates may also be used for various other applications.

The control logic can be robust and flexible. It can be totally software controlled. It will provide stable feedback when directly couple with a DAC; it can be miniaturized. The signal processing techniques can adequately handle the interference and unbalance issues. A clear understanding of the total vector can be obtained. Alignment problems are minimized and can be tackled within the filtering scheme. The control system may not demand high fidelity. A wide variety of temporal scales can be analyzed. Various signal-processing techniques can be implemented for a diverse suite of applications. A flexible, robust, sensitive low cost system will result.

One of the major objectives of the proposed effort is to develop all digital fluxgate magnetometers using the demonstrated concepts of highly sensitive analog magnetometers developed by CRS. A modern system, based on digital electronics, offers much promise in terms of eliminating the usual problems associated with analog electronics and a stable, zero-offset temperature compensated and linear system can be developed using an all-digital approach.

Use of digital electronics and improved signal processing schemes are proposed for an improved stable three-axis magnetometer. The dynamic range and the sensitivity of the basic fluxgate can be easily controlled by generating a bias field to cancel the d.c. (or the slowly varying) component of the earth's field. The bias field should be digitally controlled for improved stability and accuracy. We propose to design, develop and demonstrate an all-digital data acquisition, control and recording system for handheld applications. Temporal information of different scales is significant and should be provided in the output of the system.

Major technical challenges for the development of advanced magnetic sensors suitable for UGF application involve:

1. Development of an all-digital magnetometer to minimize noise, drift and increase stability. Increase compactness, reduced size, power consumption, etc.
2. Digital output will also allow ease of signal processing and in signal feedback. The A/D converter requirements will be relaxed.

43

3. Provide adequate alignment of the orthogonal components by using mechanical and electrical compensation techniques. This allows combination of the three orthogonal components to minimize the effects of vibration, orientation, etc.
4. Improvements in core material—reduction of Barkhausen noise, identification of noise source, use of thin films, ceramic materials or high temperature superconductors.
5. Test of sensitive magnetometer for frequencies of 1Hz and below is a significant challenge. Ambient noise fields and effects of vibrations and other interferences need to be avoided using well-shielded enclosures and using coherence estimations. Suitable techniques for necessary orthogonality of the sensor need to be developed.
6. Integration of the complete system within a miniaturized package and optimization of power and ensuring insensitivity towards environments needs to be performed.

Data Acquisition and Analysis:

Schemes for integrating the sensors with a real-time data acquisition and analysis system have been developed and a versatile system complete with sensors, data-acquisition and analysis has been designed. Plans for the experiment have been drawn.

APPENDIX B: SYNOPSIS OF VARIOUS ISSUES

Sensor Issues

Fluxgate   0 to 10 (100) Hz

Induction Coil   10 (100) Hz to 100 kHz

Passive Monitoring:

    Ferrous Metals
    Electrical activities   50 to 60 Hz, 400 Hz, several kHz
    Radio activities   450 kHz and above

External Sources

    ELF   0.1to 10 Hz, Magnetotellurics
                                        10 to 100 Hz; ELF sources
                                        (Wisconsin, Kola Peninsula, HAART – up to
                                        tens of kHz)

    VLF   Radio Stations (10 to 30 kHz)

Active Sources:

    Electrical Dipole   100 Hz to 100 kHz

    Magnetic Dipole   100 Hz to 100 kHz

1) To cover the entire band of interest, sensors from 0 Hz to several tens of kHz are needed.

2) For 0 Hz to 10 Hz: Fluxgate are sensors of choice

3) For 10 Hz and above: Induction coils are best.

4) Various sensor packages can be developed optimized for selected bands of operation

5) Performing generic design for optimized sensor design for any band of interest. Tools for such design are being developed.

Issues with Induction Coils

1) Core Material:
    Mu Metals, Permalloy, Ferrites, Metglass

2) Core Dimension:
    Length, diameter, laminations

3) Coil Parameters:
    Number of turns, wire gauge, size and type of winding, stray capacitance, internal resistance and noise, secondary coils.

4) Electronics:
    Noise Figure, Gain, phase stability, feedback parameters

5) Alignment of axis:
    Orthogonality requirements, stability

6) Shielding, RFI

7) Packaging / Gradiometric configuration

8) Signal processing and analysis

Signal Processing and Analysis:

1) A/D conversion

2) Filtering Techniques

    Removal of external noise
    Correlation and wavelets
    Coherence and wavelets
    Adaptive filtering of vibration induced effects

3) Detection and Data Presentation

Issues with Fluxgate Sensors:

Development of Digital Sensor

Alignment

Signal Acquisition

Signal Processing

Calibration

Active Systems:

    Source Development

    Waveform design

    Deployment Scenario

    Configuration

    Signal Acquisition and Processing

    Inversion

Deployment Scenarios:

    Airborne (altitude, line of flight, sampling scheme)

    Ground Deployment (sensitivity, separation, logistics)

    Unmanned Vehicles (vibration, sampling schemes)

    Underground Deployment (depth, range, source)

Excitation:

    Source of opportunity

    Electric Field Source on the ground

    B field source on the ground

    B field source in the air (collocated with receiver)

Parameters to be Measured:

In general three magnetic fields and two electric field components can be measured

In phase and quadrature components

Time and frequency measurements

Ratios between two components are convenient:

E_x/H_y	Impedance (Z)
H_z/H_x	Tipper
DH/dx	Gradient

Generalized EM Problem:
Excitation:

> Plane Wave Front from distant sources (Free space / ground)

> Spherical Wave Front from local sources (Free space / ground)

> Distorted spherical wave from local sources in ground (Free space / ground) Created by:
> Magnetic sources
> Electrical sources

Need to computed field distributions for different excitation sources at every point in the ground and above the ground. Need to use 3-D modeling. Need to perform numerical modeling for different frequencies.

These model simulations will guide us to design the sensor and also to develop the inversion techniques.

Modeling Issues:

Parameters to be measured (E, B, dB/dx, DB/dt, etc., as functions of x, y, z)

Sensitivity

Stand off distance

Ground conductivity

Frenquency range

Deployment scenarios

Modeling Limitation:

Computational Burden

Accuracies

Ground inhomogenities

Modeling Techniques:

Approximations neglecting displacement current

Approximations using diffusion type approaches

FDTD

Integral equation

FDFD (full 3-D)